

# Double heavy quarkonia production with color-octet channels at Z factory and at the CEPC/FCC-ee

Xiao-Peng Wang <sup>(a)</sup>, Guang-Zhi Xu <sup>(a),\*</sup> and Kui-Yong Liu <sup>(b)†</sup>

<sup>(a)</sup> School of Physics, Liaoning University, Shenyang 110036, China

<sup>(b)</sup> School of Physics, Liaoning Normal University, Dalian 116029, China

(Dated: January 28, 2025)

Within the NRQCD framework, we calculate the exclusive production of double heavy quarkonium(double charmonium and double bottomonium) at future super Z factory and at the CEPC/FCC-ee. The color-octet(CO) channels in the  $\gamma^*/Z^*$ -propagated process are considered along with the color-singlet(CS) channels. We found that the contributions of CO states to the total cross section are significant or dominant for many processes within energy region at Z factory and at the CEPC/FCC-ee. The experimental measurements will help us to verify the CO mechanism. Among these CO channels, the gluon fragmentation into  ${}^3S_1^8$  states is most important. Thus, the comparison between the theoretical results and future data will give a strong constraint to the matrix elements  $\langle \mathcal{O}({}^3S_1^{[8]}) \rangle$ . Additionally, we consider the relativistic corrections to both the CS and CO channels which decrease the cross sections significantly. Specially, the  $K$  factors are about 0.5 for most charmonium channels. We get estimates of the events for double heavy quarkonium production. The final events of  $J/\psi + \eta_c$ ,  $J/\psi + J/\psi$ ,  $\Upsilon + \eta_b$ ,  $\Upsilon + \Upsilon$  production would be (22, 570, 71, 61) and (206, 5343, 665, 576) at the CEPC (2-year) and at the FCC-ee (4-year) for the Z factory mode, respectively.

## I. INTRODUCTION

Heavy quarkonium is a bound state of a heavy quark ( $Q$ ) and its antiquark ( $\bar{Q}$ ) with a nonrelativistic nature. Nonrelativistic QCD (NRQCD) [1] has been widely accepted to study heavy quarkonium production and decay. Under this framework, the heavy quarkonium production can be factorized into short-distance coefficients (SDCs) and long-distance matrix elements (LDMEs). The SDCs, which represent the production of intermediate  $Q\bar{Q}$  pairs, are perturbatively calculable. The LDMEs, which are non-perturbative universal parameters, describe the hadronization of the  $Q\bar{Q}$  pair into a physical quarkonium state. These LDMEs can be obtained from potential models, lattice QCD calculations, or extracted from experimental data.

The color-octet mechanism (COM) is a key component of the NRQCD approach, introduced by systematically accounting for the higher-Fock components of a quarkonium state. Unlike the color-singlet model (CSM), the intermediate  $Q\bar{Q}$  pair in COM can be in a color-octet (CO) configuration with different quantum numbers from the final quarkonium state. With the COM, infrared divergences encountered in the CSM can be eliminated[2], and the  $\psi'$  anomaly observed at hadron colliders can be explained[3–5], which is considered a significant achievement of NRQCD. However, there are still some challenges that question the NRQCD approach. One of these is the universality problem of the CO LDMEs. LDMEs extracted from hadronic scattering measurements by different theoretical groups have shown inconsistencies[6–9]. Additionally, for inclusive and exclusive charmonium production at B factories, higher-order corrections to the color-singlet (CS) channel often saturate the data, leaving little room for the COM [10–22]. We refer the reader to the following reviews [23–27] for more information on the current status of heavy quarkonia physics.

Several future  $e^+e^-$  collider projects are proposed, including the Circular Electron Positron Collider (CEPC) [28], the Future Circular Collider (FCC) [29, 30], and the GigaZ program of the International Linear Collider (ILC) [31–34]. Additionally, a super Z factory with a high luminosity of  $\mathcal{L} \simeq 10^{34-36} \text{cm}^{-2}\text{s}^{-1}$  [35] is also proposed. These facilities provide excellent opportunities to revisit both exclusive and inclusive heavy quarkonium production, thereby allowing for a more thorough verification of the COM. Within the CSM, the exclusive production of double heavy quarkonia in  $e^+e^-$  annihilation at Z factories has been extensively studied at leading order (LO) [14, 36, 37]. Next-to-leading order (NLO) QCD corrections have also been considered [38–40]. Specifically, NLO QCD corrections for double S-wave  $B_c$  meson production [41] and associated S-wave charmonium-bottomonium production [42] have been obtained. Recently, Liao et al. [43–45] have investigated the production of double charmonia, double bottomonia, and double  $B_c$  mesons at LO. Pure QED processes also contribute observably to these production mechanisms [40]. On the other hand, it has been found that the contributions of the COM are significant in semi-exclusive processes [46]. Therefore,

\* xuguangzhi@lnu.edu.cn

† liukuiyong@lnu.edu.cn

it is also necessary to study the effects of COM in both exclusive and inclusive heavy quarkonia production processes at future  $e^+e^-$  colliders.

In the present paper, we will study the production of double heavy quarkonia (double charmonia or double bottomonia) within the COM framework. The final states for these processes include:  $J/\psi + \eta_c, J/\psi + J/\psi, J/\psi + \chi_{cJ}, J/\psi + h_c, \eta_c + \eta_c, \eta_c + h_c, \eta_c + \chi_{cJ}, \Upsilon + \eta_b, \Upsilon + \Upsilon, \Upsilon + \chi_{bJ}, \Upsilon + h_b, \eta_b + \eta_b, \eta_b + h_b, \eta_b + \chi_{bJ}$ .

The rest of this paper is organized as follows. In Section II, we present the formula and method used in our study. In Section III, we provide the input parameters and LDMEs utilized in this work. In Section IV, we analyze all possible production channels and present the results of the cross sections and differential cross sections. We also discuss the generation of events and the associated uncertainties. Finally, a summary is given in Section V.

## II. FRAMEWORK

### A. Diagrams and amplitudes

Within the NRQCD framework, the production cross sections can be divided into two parts: SDCs and LDMEs:[1]

$$\hat{\sigma}(e^+ + e^- \rightarrow H_1 + H_2) = \sum_{mn} \frac{F_{mn}}{m_{Q1}^{d_m-4} m_{Q2}^{d_n-4}} \langle 0 | \mathcal{O}_m^{H_1} | 0 \rangle \langle 0 | \mathcal{O}_n^{H_2} | 0 \rangle. \quad (1)$$

SDCs  $F_{mn}$  are labeled by the subscripts  $m$  and  $n$  for different production channels. The factor  $m_Q^{d_m, n-4}$  is introduced to make the SDCs  $F_{mn}$  dimensionless. The Fock state expansion formalism for heavy quarkonium up-to the order of  $\mathcal{O}(v^2)$  can be expressed as bellow, where  $v$  is the relative velocity between quark and anti-quark in heavy quarkonium rest frame.

$$|H\rangle = \mathcal{O}(1) |Q\bar{Q}(^{2S+1}L_J^{[1]})\rangle + \mathcal{O}(v) |Q\bar{Q}(^{2S+1}(L \pm 1)_J^{[8]})g\rangle + \mathcal{O}(v^2) |Q\bar{Q}(^{2(S \pm 1)+1}L_J^{[8]})g\rangle + \mathcal{O}(v^2) |Q\bar{Q}(^{2S+1}L_J^{[1,8]})gg\rangle + \dots \quad (2)$$

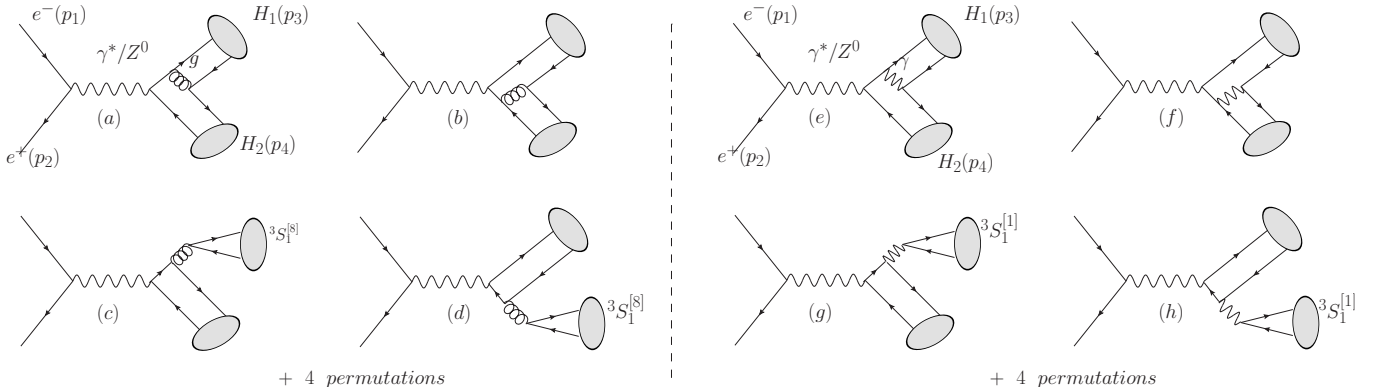


FIG. 1: CS/CO Feynman diagrams for  $e^-(p_1) + e^+(p_2) \rightarrow \gamma^*/Z^0 \rightarrow H_1(p_3) + H_2(p_4)$  at the tree level. The permutation diagrams can be obtained by reversing the quark line. The QCD diagrams are shown on the left side (a, b, c, d), and the EW diagrams are shown on the right side (e, f, g, h). (c) and (d) pertain exclusively to the CO channels. (g) and (h) pertain exclusively to the CS channels.

For specific heavy quarkonium mesons, the formula are written as,

$$|J/\psi\rangle = \mathcal{O}(1)|c\bar{c}(^3S_1^1)\rangle + \mathcal{O}(v)|c\bar{c}(^3P_J^8)g\rangle + \mathcal{O}(v^2)|c\bar{c}(^1S_0^8)g\rangle + \mathcal{O}(v^2)|c\bar{c}(^3S_1^8)gg\rangle + \dots \quad (3)$$

$$|\eta_c\rangle = \mathcal{O}(1)|c\bar{c}(^1S_0^1)\rangle + \mathcal{O}(v)|c\bar{c}(^1P_1^8)g\rangle + \mathcal{O}(v^2)|c\bar{c}(^3S_1^8)g\rangle + \mathcal{O}(v^2)|c\bar{c}(^1S_0^8)gg\rangle + \dots \quad (4)$$

$$|\chi_{cJ}\rangle = \mathcal{O}(1)|c\bar{c}(^3P_J^1)\rangle + \mathcal{O}(v)|c\bar{c}(^3S_1^8)g\rangle + \dots \quad (5)$$

$$|h_c\rangle = \mathcal{O}(1)|c\bar{c}(^1P_1^1)\rangle + \mathcal{O}(v)|c\bar{c}(^1S_0^8)g\rangle + \dots \quad (6)$$

$$|\Upsilon\rangle = \mathcal{O}(1)|b\bar{b}(^3S_1^1)\rangle + \mathcal{O}(v)|b\bar{b}(^3P_J^8)g\rangle + \mathcal{O}(v^2)|b\bar{b}(^1S_0^8)g\rangle + \mathcal{O}(v^2)|b\bar{b}(^3S_1^8)gg\rangle + \dots \quad (7)$$

$$|\eta_b\rangle = \mathcal{O}(1)|b\bar{b}(^1S_0^1)\rangle + \mathcal{O}(v)|b\bar{b}(^1P_1^8)g\rangle + \mathcal{O}(v^2)|b\bar{b}(^3S_1^8)g\rangle + \mathcal{O}(v^2)|b\bar{b}(^1S_0^8)gg\rangle + \dots \quad (8)$$

$$|\chi_{bJ}\rangle = \mathcal{O}(1)|b\bar{b}(^3P_J^1)\rangle + \mathcal{O}(v)|b\bar{b}(^3S_1^8)g\rangle + \dots \quad (9)$$

$$|h_b\rangle = \mathcal{O}(1)|b\bar{b}(^1P_1^1)\rangle + \mathcal{O}(v)|b\bar{b}(^1S_0^8)g\rangle + \dots \quad (10)$$

We will consider both the CS and CO intermediate states in the following calculations.

Our calculations include the QCD contributions (at  $\mathcal{O}(\alpha_s^2\alpha^2)$ ) and the electric-weak (EW) contributions (at  $\mathcal{O}(\alpha^4)$ ) at tree level. We employed the FeynArts[47] package to generate the Feynman diagrams and amplitudes, and utilized the FeynCalc[48] package to manipulate the amplitudes. The typical diagrams for CS and CO channels are presented in Fig. 1 through the single boson exchange process  $e^+(p_1) + e^-(p_2) \rightarrow \gamma^*/Z^*(p) \rightarrow H_1(p_3) + H_2(p_4)$ . The t-channel EW diagrams (two bosons exchange process) are not presented which give small contributions except for  $J/\psi$  pair and  $\Upsilon$  pair production. The corresponding amplitudes in perturbative QCD/EW are expressed as,

$$i\mathcal{M} = \sum_n \bar{v}(p_2)\mathcal{L}_\mu u(p_1)D^{\mu\nu}\mathcal{A}_\nu^{(n)}, \quad (11)$$

where the vertex  $\mathcal{L}^\mu$  and propagator  $D_{\mu\nu}$  are defined as,

$$\begin{aligned} \mathcal{L}^\mu &= -ie\gamma^\mu, \quad \frac{-ie}{4\cos\theta_W\sin\theta_W}\gamma^\mu(1-4\sin^2\theta_W-\gamma^5) \\ \mathcal{D}_{\mu\nu} &= \frac{-ig_{\mu\nu}}{p^2}, \quad \frac{-ig_{\mu\nu}}{p^2-m_Z^2+im_Z\Gamma_Z} \end{aligned} \quad (12)$$

In the above definitions, the first (second) term corresponds to the process propagated by  $\gamma^*$  ( $Z^0$ ).  $e = \sqrt{4\pi\alpha}$ ,  $\theta_W$  stands for the Weinberg angle, and  $m_Z$  and  $\Gamma_Z$  denote the mass and width of the  $Z^0$ -boson, respectively. In one certain channel, the hadron part of the amplitude is computed through the summation of all the diagrams, with each diagram being marked by a script, namely  $\mathcal{A}^{(n)}$ . For the  $P$ -wave state, the LO amplitude is expressed as the contraction of the orbital polarization vector  $\varepsilon(L_z)$  and the derivative of the original amplitude with respect to the relative momentum (denoted by  $q$ ) between the  $Q\bar{Q}$  pair,

$$\mathcal{A} = \varepsilon^\rho(L_z)\frac{\partial}{\partial q^\rho}\tilde{\mathcal{A}}|_{q\rightarrow 0} \quad (13)$$

Through the projection operator method,  $Q\bar{Q}$  is projected onto specific spin and color quantum numbers. For instance, the original amplitudes of the diagrams labeled (a) and (c) in Fig. 1 are written as below,

$$\begin{aligned} \tilde{\mathcal{A}}_\nu^{(a)} &= g^2\text{Tr}\left[\Pi_1\gamma_\rho\frac{(\not{p}_{3Q}+\not{p}_{3\bar{Q}}+\not{p}_{4Q})+m_Q}{[(p_{3Q}+p_{3\bar{Q}}+p_{4Q})^2-m_Q^2](p_{3\bar{Q}}+p_{4Q})^2}\mathcal{V}_\nu\Pi_2\gamma^\rho\right] \\ \tilde{\mathcal{A}}_\nu^{(c)} &= -g^2\text{Tr}\left[\gamma^\rho\Pi_1\right]\text{Tr}\left[\Pi_2\gamma_\rho\frac{(\not{p}_{3Q}+\not{p}_{3\bar{Q}}+\not{p}_{4Q})+m_Q}{[(p_{3Q}+p_{3\bar{Q}}+p_{4Q})^2-m_Q^2](p_{3Q}+p_{3\bar{Q}})^2}\mathcal{V}_\nu\right] \end{aligned} \quad (14)$$

The phase difference between the two amplitudes with a sign change arises because one diagram can be obtained by exchanging the identical final-state fermions in the other. The vertex  $\mathcal{V}_\nu$  for  $\gamma/Z$  propagation are defined as follows,

$$\mathcal{V}_\nu = iee_Q\gamma_\nu, \quad \frac{ie}{4\cos\theta_W\sin\theta_W}\gamma_\nu(1-4|e_Q|\sin^2\theta_W-\gamma^5) \quad (15)$$

where  $e_Q$  is the charge of heavy quark. The projection operator  $\Pi_i$ , with the subscript  $i$  indicating the specific states, is constituted as the multiplicative combination of the spin projection and the color projection. The expressions of

spin-singlet and spin-triplet projection operators are,

$$\Pi(00) \equiv \sum_{s_Q s_{\bar{Q}}} \langle s_Q s_{\bar{Q}}; 00 \rangle v(p_{\bar{Q}}) \bar{u}(p_Q) = \frac{1}{2\sqrt{2}(E_q + m_Q)} (-\not{p}_{\bar{Q}} + m_Q) \gamma_5 \frac{\not{p}_Q + \not{p}_{\bar{Q}} + 2E_q}{2E_q} (\not{p}_Q + m_Q) \quad (16)$$

$$\Pi(1s_z) \equiv \sum_{s_Q s_{\bar{Q}}} \langle s_Q s_{\bar{Q}}; 1s_z \rangle v(p_{\bar{Q}}) \bar{u}(p_Q) = \frac{1}{2\sqrt{2}(E_q + m_Q)} (-\not{p}_{\bar{Q}} + m_Q) \not{\epsilon}(s_z) \frac{\not{p}_Q + \not{p}_{\bar{Q}} + 2E_q}{2E_q} (\not{p}_Q + m_Q) \quad (17)$$

where  $\varepsilon(L_z)$  is the spin polarization vector,  $E_q$  is the total energy of quark or antiquark in the rest frame of the meson. Color projection operators assume the form of  $\sum_{ij} \frac{\delta_{ij}}{\sqrt{N_c}}$  in the case of CS, and  $\sqrt{2}T_{ij}^a$ ,  $a = 1, 2, \dots, 8$  for CO.

The requirement for the overall colorless nature of the final state dictates that both particles must be either in the CS state or in the CO state. For the CS channel, the color factors of diagram (a) and (b) are  $\frac{N_c^2 - 1}{2N_c}$ , while for the CO channel, they are  $-\frac{\delta_{ab}}{2N_c}$  where  $a, b$  are the color indexes of final states. In contrast, diagrams (c) and (d) can only be in the CO state, and the gluon fragment into the  ${}^3S_1^{[8]}$  state. The total color factors are  $\frac{\delta_{ab}}{2}$ . For the CS channel, the color factors of diagram (e) and (f) are 1, while for the CO channel, they are  $\delta_{ab}$ . Diagrams (c) and (d) can only be in the CS state, and the final  $\gamma^*/Z^0$  fragment into the  ${}^3S_1^{[1]}$  state. The total color factors are  $N_c$ .

## B. Kinematics and relativistic corrections (RCs)

We compute the cross sections of each channel up to the NLO of  $\mathcal{O}(v^2)$  and the conventional approach is employed to derive the RCs, as referenced in [13, 17–19, 49, 50]. For the  $S$ -wave state, the amplitudes are expanded to the second order of  $|\vec{q}|$ , whereas for the  $P$ -wave state, the expansion is carried out to the third order. Here,  $|\vec{q}|$  which is a Lorentz scalar represents the magnitude of the three-momentum of either  $Q$  or  $\bar{Q}$  within the rest frame of the meson. Consequently, we have  $E_q = \sqrt{m_Q^2 + \vec{q}^2}$  and the meson mass can be approximated as  $2E_q$ . The momentum of  $Q(\bar{Q})$  in arbitrary frame is expressed as  $p_Q = \frac{1}{2}p + q$  ( $p_{\bar{Q}} = \frac{1}{2}p - q$ ) where  $q$  is obtained via Lorentz boost from  $(0, \vec{q})$ . Therefore, after integrating out the angles of  $q$ , the corresponding relationship between the polynomial term of  $q$  and  $|\vec{q}|^2$  can be ascertained.  $q^\alpha q^\beta \rightarrow \frac{|\vec{q}|^2}{3} \pi^{\alpha\beta}$  for  $S$ -wave state,  $q^\alpha q^\beta q^\sigma \rightarrow \frac{|\vec{q}|^3}{5} (\pi^{\alpha\beta} \varepsilon_{L_z}^\sigma + \pi^{\alpha\sigma} \varepsilon_{L_z}^\beta + \pi^{\beta\sigma} \varepsilon_{L_z}^\alpha)$  for  $P$ -wave state, where  $\pi^{\alpha\beta} = -g^{\alpha\beta} + \frac{p^\alpha p^\beta}{p^2}$ . Furthermore, the normalization factor of  $\sqrt{\frac{m_Q}{E_q}}$  is incorporated into the amplitudes.

The kinematics variables should be also expanded. For two-body final states, the Lorentz invariant Mandelstam variables are defined as,

$$s = (p_1 + p_2)^2 = (p_3 + p_4)^2, t = (p_3 - p_1)^2 = (p_4 - p_2)^2, u = (p_4 - p_1)^2 = (p_3 - p_2)^2. \quad (18)$$

with the relationship  $s + t + u = M_{H_1}^2 + M_{H_2}^2$ . The variable  $s$  is independent of  $|\vec{q}|^2$ , while  $t$  and  $u$  are dependent on  $|\vec{q}|^2$ . We define  $t_0$  as the value of  $t$  when  $|\vec{q}_1| = |\vec{q}_2| = 0$ , and  $u_0$  as the value of  $u$  when  $|\vec{q}_1| = |\vec{q}_2| = 0$ . Consequently, the following expansions are derived, as presented in [49].

$$t = t_0 - \frac{4[t_0 + 4m_Q^2]}{s - 16m_Q^2} (|\vec{q}_1|^2 + |\vec{q}_2|^2) + \mathcal{O}(v^4) \quad (19)$$

$$u = u_0 - \frac{4[u_0 + 4m_Q^2]}{s - 16m_Q^2} (|\vec{q}_1|^2 + |\vec{q}_2|^2) + \mathcal{O}(v^4) \quad (20)$$

The matrix elements of  $\langle v^2 \rangle$  are defined by the ratios of the NLO LDMEs in  $v^2$  to the LO LDMEs,

$$\langle v^2 \rangle \equiv \frac{\langle 0 | \mathcal{P}^H(2s+1)L_J | 0 \rangle}{m_Q^2 \langle 0 | \mathcal{O}^H(2s+1)L_J | 0 \rangle} \quad (21)$$

which adhere to the velocity power scaling rules and are of the order of  $v^2$ . Moreover,

$$v^2 = \langle v^2 \rangle [1 + \mathcal{O}(v^4)] \quad (22)$$

The four-Fermion operators  $\mathcal{O}^H(2s+1)L_J$ , which are of dimension-6 for the LO, and the dimension-8 four-Fermion operators  $\mathcal{P}^H(2s+1)L_J$  utilized for the RCs, are defined in accordance with Ref. [1].

### III. PARAMETERS

We will take the following input parameters[51] and LDMEs[52] in the present work,

$$\begin{aligned} \alpha_s(2m_c) &= 0.26, \quad \alpha_s(2m_b) = 0.18, \quad \alpha = 1/137, \\ m_c &= 1.5 \text{ GeV}, \quad m_b = 4.7 \text{ GeV}, \quad m_Z = 91.1876 \text{ GeV}, \\ \Gamma_Z &= 2.4952 \text{ GeV}, \quad \sin^2 \theta_w = 0.2312, \quad v_{cc}^2 = 0.23, \quad v_{bb}^2 = 0.1, \end{aligned} \quad (23)$$

Here, the strong running coupling constant  $\alpha_s$  is calculated by the two-loop formula,

$$\frac{\alpha_s(\mu)}{4\pi} = \frac{1}{\beta_0 L} - \frac{\beta_1 \ln L}{\beta_0^3 L^2} \quad (24)$$

where  $L = \ln(\mu^2/\Lambda_{QCD}^2)$  with  $\Lambda_{QCD} \simeq 338 \text{ MeV}$ ,  $\beta_0 = (11/3)C_A - (4/3)T_f n_f$  and  $\beta_1 = (34/3)C_A^2 - 4C_F T_f n_f - (20/3)C_A T_f$  are the one-loop and two-loop coefficients of the QCD beta function, respectively.  $n_f$  is the active quark flavors which is set to 3 for heavy quarkonia. The values of  $v^2$  for CS and CO are estimated via the Gremm-Kapustin relation[53, 54],

$$v^2 = v_1^2 = v_8^2 = \frac{M_{Q\bar{Q}} - 2m_Q^{pole}}{m_Q^{QCD}} \quad (25)$$

where  $m_Q^{pole}$  is quark pole mass,  $m_Q^{QCD}$  is the quark mass in NRQCD,  $M_{Q\bar{Q}}$  is heavy quarkonium mass.

The LDMEs of charmonium[55–63] are,

$$\begin{aligned} \langle \mathcal{O}^{J/\psi} [^3S_1^{[1]}] \rangle &= 1.2 \text{ GeV}^3 \\ \langle \mathcal{O}^{J/\psi} [^1S_0^{[8]}] \rangle &= 0.0180 \pm 0.0087 \text{ GeV}^3 \\ \langle \mathcal{O}^{J/\psi} [^3S_1^{[8]}] \rangle &= 0.0013 \pm 0.0013 \text{ GeV}^3 \\ \langle \mathcal{O}^{J/\psi} [^3P_0^{[8]}] \rangle &= (0.0180 \pm 0.0087)m_c^2 \text{ GeV}^3 \end{aligned} \quad (26)$$

$$\begin{aligned} \langle \mathcal{O}^{\eta_c} [^1S_0^{[1]}] \rangle &= \frac{1}{3} \times 1.2 \text{ GeV}^3 \\ \langle \mathcal{O}^{\eta_c} [^1S_0^{[8]}] \rangle &= \frac{1}{3} \times (0.0013 \pm 0.0013) \text{ GeV}^3 \\ \langle \mathcal{O}^{\eta_c} [^3S_1^{[8]}] \rangle &= 0.0180 \pm 0.0087 \text{ GeV}^3 \\ \langle \mathcal{O}^{\eta_c} [^1P_1^{[8]}] \rangle &= 3 \times (0.0180 \pm 0.0087)m_c^2 \text{ GeV}^3 \end{aligned}$$

$$\begin{aligned} \langle \mathcal{O}^{h_c} [^1P_1^{[1]}] \rangle &= 3 \times 0.054m_c^2 \text{ GeV}^3 \\ \langle \mathcal{O}^{h_c} [^1S_0^{[8]}] \rangle &= 3 \times (0.00187 \pm 0.00025) \text{ GeV}^3 \end{aligned}$$

$$\begin{aligned} \langle \mathcal{O}^{\chi_{c0}} [^3P_0^{[1]}] \rangle &= 0.054m_c^2 \text{ GeV}^3 \\ \langle \mathcal{O}^{\chi_{c0}} [^3S_1^{[8]}] \rangle &= 0.00187 \pm 0.00025 \text{ GeV}^3 \\ \langle \mathcal{O}^{\chi_{c1}} [^3P_1^{[1]}] \rangle &= 3 \times 0.054m_c^2 \text{ GeV}^3 \\ \langle \mathcal{O}^{\chi_{c1}} [^3S_1^{[8]}] \rangle &= 3 \times (0.00187 \pm 0.00025) \text{ GeV}^3 \\ \langle \mathcal{O}^{\chi_{c2}} [^3P_2^{[1]}] \rangle &= 5 \times 0.054m_c^2 \text{ GeV}^3 \\ \langle \mathcal{O}^{\chi_{c2}} [^3S_1^{[8]}] \rangle &= 5 \times (0.00187 \pm 0.00025) \text{ GeV}^3 \end{aligned}$$

and that of bottomonium[55, 56, 62–64] are:

$$\begin{aligned} \langle \mathcal{O}^{\Upsilon} [^3S_1^{[1]}] \rangle &= 10.9 \text{ GeV}^3 \\ \langle \mathcal{O}^{\Upsilon} [^1S_0^{[8]}] \rangle &= (0.0121 \pm 0.0400) \text{ GeV}^3 \\ \langle \mathcal{O}^{\Upsilon} [^3S_1^{[8]}] \rangle &= (0.0477 \pm 0.0334) \text{ GeV}^3 \\ \langle \mathcal{O}^{\Upsilon} [^3P_0^{[8]}] \rangle &= 5 \times (0.0121 \pm 0.0400)m_b^2 \text{ GeV}^3 \end{aligned}$$

$$\begin{aligned}
\langle \mathcal{O}^{\chi_{b0}} [{}^3P_0^{[1]}] \rangle &= 0.1m_b^2 \text{ GeV}^3 \\
\langle \mathcal{O}^{\chi_{b0}} [{}^3S_1^{[8]}] \rangle &= 0.1008 \text{ GeV}^3 \\
\langle \mathcal{O}^{\chi_{b1}} [{}^3P_1^{[1]}] \rangle &= 3 \times 0.1m_b^2 \text{ GeV}^3 \\
\langle \mathcal{O}^{\chi_{b1}} [{}^3S_1^{[8]}] \rangle &= 3 \times 0.1008 \text{ GeV}^3 \\
\langle \mathcal{O}^{\chi_{b2}} [{}^3P_2^{[1]}] \rangle &= 5 \times 0.1m_b^2 \text{ GeV}^3 \\
\langle \mathcal{O}^{\chi_{b2}} [{}^3S_1^{[8]}] \rangle &= 5 \times 0.1008 \text{ GeV}^3
\end{aligned}$$

$$\begin{aligned}
\langle \mathcal{O}^{\eta_b} [{}^1S_0^{[1]}] \rangle &= \frac{1}{3} \langle \mathcal{O}^{\Upsilon} [{}^3S_1^{[1]}] \rangle = 3.633 \text{ GeV}^3 \\
\langle \mathcal{O}^{\eta_b} [{}^1S_0^{[8]}] \rangle &= \frac{1}{3} \langle \mathcal{O}^{\Upsilon} [{}^3S_1^{[8]}] \rangle = (0.0159 \pm 0.0111) \text{ GeV}^3 \\
\langle \mathcal{O}^{\eta_b} [{}^3S_1^{[8]}] \rangle &= \langle \mathcal{O}^{\Upsilon} [{}^1S_0^{[8]}] \rangle = (0.0121 \pm 0.0400) \text{ GeV}^3 \\
\langle \mathcal{O}^{\eta_b} [{}^1P_1^{[8]}] \rangle &= 3 \times \langle \mathcal{O}^{\Upsilon} [{}^3P_0^{[8]}] \rangle = 3 \times 5 \times (0.0121 \pm 0.0400)m_b^2 \text{ GeV}^3
\end{aligned}$$

$$\begin{aligned}
\langle \mathcal{O}^{h_b} [{}^1P_1^{[1]}] \rangle &= 3 \times \langle \mathcal{O}^{\chi_{b0}} [{}^3P_0^{[1]}] \rangle = 3 \times 0.1m_b^2 \text{ GeV}^3 \\
\langle \mathcal{O}^{h_b} [{}^1S_0^{[8]}] \rangle &= 3 \times \langle \mathcal{O}^{\chi_{b0}} [{}^3S_1^{[8]}] \rangle = 3 \times 0.1008 \text{ GeV}^3
\end{aligned}$$

The heavy quark spin symmetry (HQSS) is exhibited by them [1]:

$$\begin{aligned}
\langle \mathcal{O}^{\chi_{cJ}} [{}^3P_J^{[1]}] \rangle &= (2J+1) \langle \mathcal{O}^{\chi_{c0}} [{}^3P_0^{[1]}] \rangle \\
\langle \mathcal{O}^{\chi_{cJ}} [{}^3S_1^{[8]}] \rangle &= (2J+1) \langle \mathcal{O}^{\chi_{c0}} [{}^3S_1^{[8]}] \rangle \\
\langle \mathcal{O}^{\eta_c} [{}^1S_0^{[1]}/{}^1S_0^{[8]}] \rangle &= \frac{1}{3} \langle \mathcal{O}^{J/\psi} [{}^3S_1^{[1]}/{}^3S_1^{[8]}] \rangle, \langle \mathcal{O}^{\eta_c} [{}^3S_1^{[8]}] \rangle = \langle \mathcal{O}^{J/\psi} [{}^1S_0^{[8]}] \rangle \\
\langle \mathcal{O}^{\eta_c} [{}^1P_1^{[8]}] \rangle &= 3 \langle \mathcal{O}^{J/\psi} [{}^3P_0^{[8]}] \rangle, \langle \mathcal{O}^{h_c} [{}^1P_1^{[1]}/{}^1S_0^{[8]}] \rangle = 3 \langle \mathcal{O}^{\chi_{c0}} [{}^3P_0^{[1]}/{}^3S_1^{[8]}] \rangle
\end{aligned} \tag{27}$$

we also see that these parameters approximately satisfy the velocity scaling rule (VSR) of NRQCD[1],

$$\begin{aligned}
\langle \mathcal{O}^{J/\psi} [{}^3S_1^{[1]}] \rangle &\sim m_c^3 v_c^3, \langle \mathcal{O}^{\chi_{cJ}} [{}^3P_J^{[1]}] \rangle \sim m_c^5 v_c^5, \\
\langle \mathcal{O}^{J/\psi} [{}^3S_1^{[8]}] \rangle &\sim m_c^3 v_c^7, \langle \mathcal{O}^{\chi_{cJ}} [{}^3S_1^{[8]}] \rangle \sim m_c^3 v_c^5, \\
&\dots\dots
\end{aligned} \tag{28}$$

the CS LDMEs satisfy the quark potential model[1],

$$\begin{aligned}
\frac{\langle \mathcal{O}^{J/\psi} [{}^3S_1^{[1]}] \rangle}{2N_c \times 3} &\simeq \frac{|R_S(0)|^2}{4\pi}, \frac{\langle \mathcal{O}^{\eta_c} [{}^1S_0^{[1]}] \rangle}{2N_c} \simeq \frac{|R_S(0)|^2}{4\pi} \\
\frac{\langle \mathcal{O}^{\chi_{cJ}} [{}^3P_J^{[1]}] \rangle}{2N_c(2J+1)} (J=0,1,2) &\simeq \frac{3|R'_P(0)|^2}{4\pi}, \frac{\langle \mathcal{O}^{h_c} [{}^1P_1^{[1]}] \rangle}{2N_c \times 3} \simeq \frac{3|R'_P(0)|^2}{4\pi}
\end{aligned} \tag{29}$$

The CS LDMEs of charmonia used in this work, which correspond to the values of  $|R_s(0)|^2 = 0.838$ ,  $|R'_p(0)|^2 = 0.085$ , are closely approximate the value ( $|R_s(0)|^2 = 0.810$ ,  $|R'_p(0)|^2 = 0.075$ ) in Ref. [65], compared to maximal ( $|R_s(0)|^2 = 2.458$ ,  $|R'_p(0)|^2 = 0.322$ [66]) and minimal ( $|R_s(0)|^2 = 0.565$ ,  $|R'_p(0)|^2 = 0.053$ [67]) set in Refs. [43, 68], and that of bottomonia ( $|R_s(0)|^2 = 7.61$ ,  $|R'_p(0)|^2 = 1.54$ ) are closely approximate the value ( $|R_s(0)|^2 = 6.477$ ,  $|R'_p(0)|^2 = 1.417$ ) in Ref. [65], compared to maximal ( $|R_s(0)|^2 = 16.12$ ,  $|R'_p(0)|^2 = 5.874$ [66]) and minimal ( $|R_s(0)|^2 = 5.298$ ,  $|R'_p(0)|^2 = 1.111$ [69]) set in Refs. [43, 68].

Analogous correlations among the LDMEs are also valid for bottomonia.

## IV. RESULTS AND DISCUSSION

### A. Cross sections and CO contributions

In the energy region of Z-factory, the pure EW contributions are also significant[40]. For the  $J/\psi$  pair and  $\Upsilon$  pair production, we consider the t-channel EW contributions which are significant either at B-factory or at the Z-factory[70–72]. For other processes, the t-channel EW contributions could be neglected compared with the s-channel

contributions. The  $\gamma^*$ -propagated processes contribute predominantly at the B-factory, but are negligible compared with the  $Z^0$ -propagated processes in the energy region of the Z-factory. And for the  $\gamma^*$ -propagated processes, due to the additional C-parity conservation constraint imposed by the  $\gamma^*$  propagator, these processes exhibit fewer production channels. Therefore, in our calculations, the total cross sections will include the complete contributions from QCD and EW processes, as well as  $\gamma^*/Z^0$ -propagated processes. The interferences were also taken into account.

In Table I, we present the contributions stemming from all combinations of the CS and CO states that comply with the conservation laws of color, C-parity, and combined CP-parity. Upon examining the table, it becomes evident that the CO channels contribute substantially more than the CS channels in several processes, particularly for the combinations involving the  $^3S_1^{[8]}$  state. This indicates that the processes of gluon fragmentation into the intermediate  $^3S_1^{[8]}$  state might play a crucial role. The significance of the  $^3S_1^{[8]}$  state has also been emphasized in Refs. [46, 73], where the semi-exclusive heavy quarkonia production and the inclusive  $\eta_Q$  production at the Z-factory were investigated.

The cross-sections vary with centre-of-mass (c.m.) energy  $\sqrt{s}$  are presented in Figs. 2 and 3. In the energy region of the B factory,  $\gamma^*$  propagation process dominates. Near the energy of the  $Z^0$  pole,  $Z^0$  propagation process dominates due to the resonance effects. Differing from the case in B factory where the production of double charmonium is mainly due to the color singlet mechanism with the color octet contribution being negligible, at the Z factories, the color octet contribution prevails in a number of production processes. In Figs. 4, 5, the ratios  $\sigma_{CO}/\sigma_{Total}$  versus  $\sqrt{s}$  have been illustrated, enabling a more direct and intuitive perception of the color octet contributions to the total cross sections. It should be noted that in the production of double  $\eta_c$  or double  $\eta_b$ , the contributions stemming from the CS channels vanish when the  $t$ -channel is left out of consideration.

Relativistic corrections (RCs) exert a substantial impact on double charmonia production. At the  $Z^0$  pole and for higher collision energies, the  $K$  factors associated with the NLO( $v^2$ ) cross sections falls within the range of  $0.3 \sim 0.5$ . And for bottomonia production, the influence of RCs is relatively minor. Here, the  $K$  factor is in the range of  $0.7 \sim 0.8$ . In Appendix VI, we depict the ratios of  $\sigma_{NLO(v^2)}/\sigma_{LO}$  (i.e., the  $K$  factors) as a function of  $\sqrt{s}$  in Figs. 13 and 14. Correspondingly, in Appendix VII, we elucidate the ratios of the SDCs corresponding to the RCs and those at LO in the large energy limit. Notably, the NLO QCD corrections can also be remarkably significant, with the  $K$  factor reaching as high as  $2 \sim 5$ , as reported in [38, 40].



TABLE I: Production channels and corresponding cross sections (units:  $\times 10^{-4} fb$ ) at  $Z^0$  pole in  $\mathcal{O}(v^0)$ . The percentage inside the brackets is the proportion of CO. The negligible results ( $< 0.1 \times 10^{-4} fb$ ) are not shown.

$H_1$		$H_2$								
charmonia										
$\eta_c$	$J/\psi$	32.1 (66.1%)	$\chi_{cJ}$	11.9( $J=0$ ) (42.7%)	16.1( $J=1$ ) (95.0%)	39.5( $J=2$ ) (64.3%)	$h_c$	4.4 (31.0%)	$\eta_c$	39.2 (100.0%)
$^1S_0^{[1]}$	$^3S_1^{[1]}$	10.9	$^3P_J^{[1]}$	6.8	0.8	14.1	$^1P_1^{[1]}$	3.1	$^1S_0^{[1]}$	
$^3S_1^{[8]}$	$^1S_0^{[8]}$	4.4	$^3S_1^{[8]}$	2.0	6.1	10.2	$^1S_0^{[8]}$	1.4	$^3S_1^{[8]}$	9.8
	$^3S_1^{[8]}$	1.4								
	$^3P_J^{[8]}$	13.2								
$^1S_0^{[8]}$	$^3S_1^{[8]}$		$^3S_1^{[8]}$			0.1			$^3S_1^{[8]}$	0.1
	$^3P_J^{[8]}$								$^1P_1^{[8]}$	
$^1P_1^{[8]}$	$^1S_0^{[8]}$		$^3S_1^{[8]}$	3.0	9.1	15.2	$^1S_0^{[8]}$		$^3S_1^{[8]}$	29.3
	$^3S_1^{[8]}$	2.1							$^1P_1^{[8]}$	
	$^3P_J^{[8]}$									
$J/\psi$	$J/\psi$	2737.4 (0.1%)	$\chi_{cJ}$	4.1( $J=0$ ) (48.4%)	8.2( $J=1$ ) (72.5%)	13.1( $J=2$ ) (75.7%)	$h_c$	33.3 (0.3%)		
$^3S_1^{[1]}$	$^3S_1^{[1]}$	2736.0	$^3P_J^{[1]}$	2.1	2.3	3.2	$^1P_1^{[1]}$	33.2		
$^3S_1^{[8]}$	$^3S_1^{[8]}$	0.1	$^3S_1^{[8]}$	0.1	0.4	0.7	$^1S_0^{[8]}$	0.1		
$^1S_0^{[8]}$	$^3P_J^{[8]}$		$^3S_1^{[8]}$	0.5	1.4	2.3				
	$^3S_1^{[8]}$	0.3								
$^3P_J^{[8]}$	$^3P_J^{[8]}$		$^3S_1^{[8]}$	1.4	4.1	6.9	$^1S_0^{[8]}$			
	$^3S_1^{[8]}$	0.9								
bottomonia										
$\eta_b$	$\Upsilon$	37.6 (5.2%)	$\chi_{bJ}$	8.1( $J=0$ ) (37.7%)	15.0( $J=1$ ) (60.7%)	28.5( $J=2$ ) (53.3%)	$h_b$	7.8 (9.6%)	$\eta_b$	0.3 (100.0%)
$^1S_0^{[1]}$	$^3S_1^{[1]}$	35.7	$^3P_J^{[1]}$	5.0	5.9	13.3	$^1P_1^{[1]}$	7.1	$^1S_0^{[1]}$	
$^3S_1^{[8]}$	$^1S_0^{[8]}$		$^3S_1^{[8]}$	0.3	1.0	1.6	$^1S_0^{[8]}$	0.7	$^3S_1^{[8]}$	
	$^3S_1^{[8]}$	0.2								
	$^3P_J^{[8]}$	0.4								
$^1S_0^{[8]}$	$^3S_1^{[8]}$	0.2	$^3S_1^{[8]}$	0.3	1.0	1.6			$^3S_1^{[8]}$	
	$^3P_J^{[8]}$								$^1P_1^{[8]}$	
$^1P_1^{[8]}$	$^1S_0^{[8]}$		$^3S_1^{[8]}$	2.4	7.2	12.0	$^1S_0^{[8]}$		$^3S_1^{[8]}$	0.3
	$^3S_1^{[8]}$	1.1							$^1P_1^{[8]}$	
	$^3P_J^{[8]}$									
	$^3S_1^{[8]}$									
$\Upsilon$	$\Upsilon$	36.7 (6.1%)	$\chi_{bJ}$	13.3( $J=0$ ) (39.6%)	17.1( $J=1$ ) (92.4%)	32.9( $J=2$ ) (80.0%)	$h_b$	25.2 (11.7%)		
$^3S_1^{[1]}$	$^3S_1^{[1]}$	34.4	$^3P_J^{[1]}$	8.0	1.3	6.6	$^1P_1^{[1]}$	22.2		
$^3S_1^{[8]}$	$^3S_1^{[8]}$	0.3	$^3S_1^{[8]}$	1.3	3.9	6.5	$^1S_0^{[8]}$	2.9		
$^1S_0^{[8]}$	$^3P_J^{[8]}$		$^3S_1^{[8]}$	0.2	0.7	1.2				
	$^3S_1^{[8]}$	0.1								
$^3P_J^{[8]}$	$^3P_J^{[8]}$	0.1	$^3S_1^{[8]}$	3.7	11.2	18.7	$^1S_0^{[8]}$	0.1		
	$^3S_1^{[8]}$	1.8								

The numerical results of the total cross section at  $\sqrt{s} = m_Z$  are illustrated in Table II. For comparison, we present the total cross sections of CS as well as CS plus CO, at the order of  $v^0$  and  $v^2$ , respectively. Our LO CS results are in agreement with Refs. [12, 36, 40, 43, 74] when using the same input parameters. <sup>1</sup> Our NLO( $v^2$ ) CS result of  $\gamma^* \rightarrow J/\psi + \eta_c$  are consistent with Ref. [17].

<sup>1</sup> We find that a few processes are in contradiction with Ref. [43], our results of  $\sigma(J/\psi + J/\psi)_{Z^0}$  ( $\sigma(\Upsilon + \Upsilon)_{Z^0}$ ) are half of those in Ref. [43], and the difference might be due to the particle identities. Moreover, in our results,  $\sigma(J/\psi + h_c)_{\gamma^*}$  and  $\sigma(\Upsilon + h_b)_{\gamma^*}$  are zero because of the C-parity conservation, which are also different from the values in Ref. [43].



TABLE II: Production cross sections (units: $\times 10^{-4}$  fb) of the double heavy quarkonia at  $\sqrt{s}=91.1876$  GeV. LO and NLO( $v^2$ ) mean leading order and next-to-leading order results in the  $v^2$  expansions, respectively. CS means the cross section of color-singlet channel, and CO means cross sections of all the color-octet channels.

	charmonia				bottomonia				
	CS		CS+CO		CS		CS+CO		
	LO	NLO( $v^2$ )	LO	NLO( $v^2$ )	LO	NLO( $v^2$ )	LO	NLO( $v^2$ )	
$J/\psi + J/\psi$	2736.0	355.7	2737.4	356.2	$\Upsilon + \Upsilon$	34.4	36.8	36.7	38.4
$J/\psi + \eta_c$	10.9	6.2	32.1	13.7	$\Upsilon + \eta_b$	35.7	43.0	37.6	44.3
$J/\psi + h_c$	33.2	20.2	33.3	20.3	$\Upsilon + h_b$	22.2	20.4	25.2	22.5
$J/\psi + \chi_{c0}$	2.1	1.4	4.1	2.1	$\Upsilon + \chi_{b0}$	8.0	7.9	13.3	11.7
$J/\psi + \chi_{c1}$	2.3	0.9	8.2	3.0	$\Upsilon + \chi_{b1}$	1.3	1.5	17.1	12.9
$J/\psi + \chi_{c2}$	3.2	2.3	13.1	5.9	$\Upsilon + \chi_{b2}$	6.6	6.4	32.9	25.4
$\eta_c + \eta_c$	0.0	0.0	39.2	13.3	$\eta_b + \eta_b$	0.0	0.0	0.3	0.2
$\eta_c + h_c$	3.1	1.5	4.4	2.1	$\eta_b + h_b$	7.1	5.5	7.8	6.0
$\eta_c + \chi_{c0}$	6.8	3.4	11.9	5.4	$\eta_b + \chi_{b0}$	5.0	3.8	8.1	5.9
$\eta_c + \chi_{c1}$	0.8	1.1	16.1	6.8	$\eta_b + \chi_{b1}$	5.9	6.7	15.0	12.8
$\eta_c + \chi_{c2}$	14.1	9.4	39.5	19.0	$\eta_b + \chi_{b2}$	13.3	12.1	28.5	22.4

In Figs. 7 and 8, we depict the differential cross section  $d\sigma/d\cos\theta$ , where  $\theta$  denotes the scattering angle of  $H_1$ . It is evident that within the CS channel, a concave distribution pattern emerges for  $J/\psi + \eta_c/\chi_{c1}/J/\psi, \eta_c + \chi_{c1}$  and  $\Upsilon + \eta_b/\chi_{b1}/\Upsilon, \eta_b + \chi_{b1}$ . In contrast, the remaining processes within this channel exhibit a bulge distribution. As for the total CO channel, a concave distribution is characteristic of all its processes.

The differential cross section  $\frac{d\sigma}{dp_t}$  can be written as:

$$\frac{d\sigma}{dp_t} = \left| \frac{d\cos\theta}{dp_t} \right| \left( \frac{d\sigma}{d\cos\theta} \right) = \frac{p_t}{|\vec{p}_3| \sqrt{p_3^2 - p_t^2}} \left( \frac{d\sigma}{d\cos\theta} \right) \quad (30)$$

and the momentum of the  $H_1$  heavy quarkonia:

$$\vec{p}_3 = \frac{\sqrt{\lambda[s, (2E_{q3})^2, (2E_{q4})^2]}}{2\sqrt{s}} \quad (31)$$

Combining the Eqs. (30) and (31), we can also get a  $\mathcal{O}(v^2)$  expression:

$$\frac{d\sigma}{dp_t} = \frac{4p_t s^{3/2} [s(s - 4p_t^2) - 16m_Q^2(2p_t^2 - s)(v^2 - 2) - 256m_Q^4(v^2 - 1)]}{[s(s - 16m_Q^2)]^{3/2} (s - 16m_Q^2 - 4p_t^2)^{3/2}} \left( \frac{d\sigma}{d\cos\theta} \right) + \mathcal{O}(v^4) \quad (32)$$

The results are shown in Figs. 9 and 10, it's seen that the  $p_t$  distribution change is more stable for the CO channel than for the CS channel.

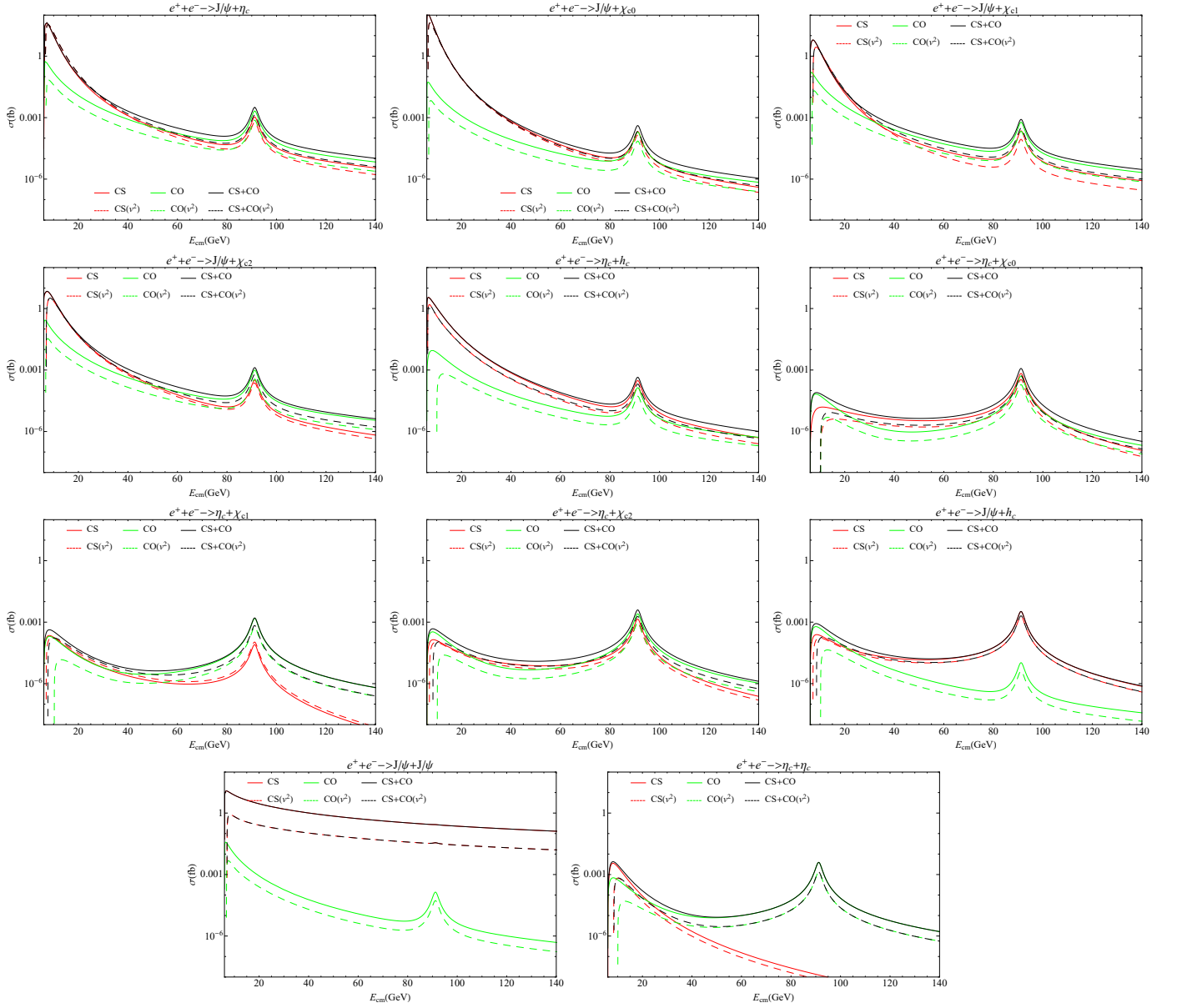


FIG. 2: (Color online) Cross sections ( $\sigma$ ) versus c.m. energy ( $E_{cm} = \sqrt{s}$ ) for double charmonium production. The solid line represents leading order (LO) and the dashed line represents next-to-leading order in  $v^2$  (NLO) results. The red line represents the CS channel, the green line represents the total CO channels and the black line represents the sum of CS and CO.

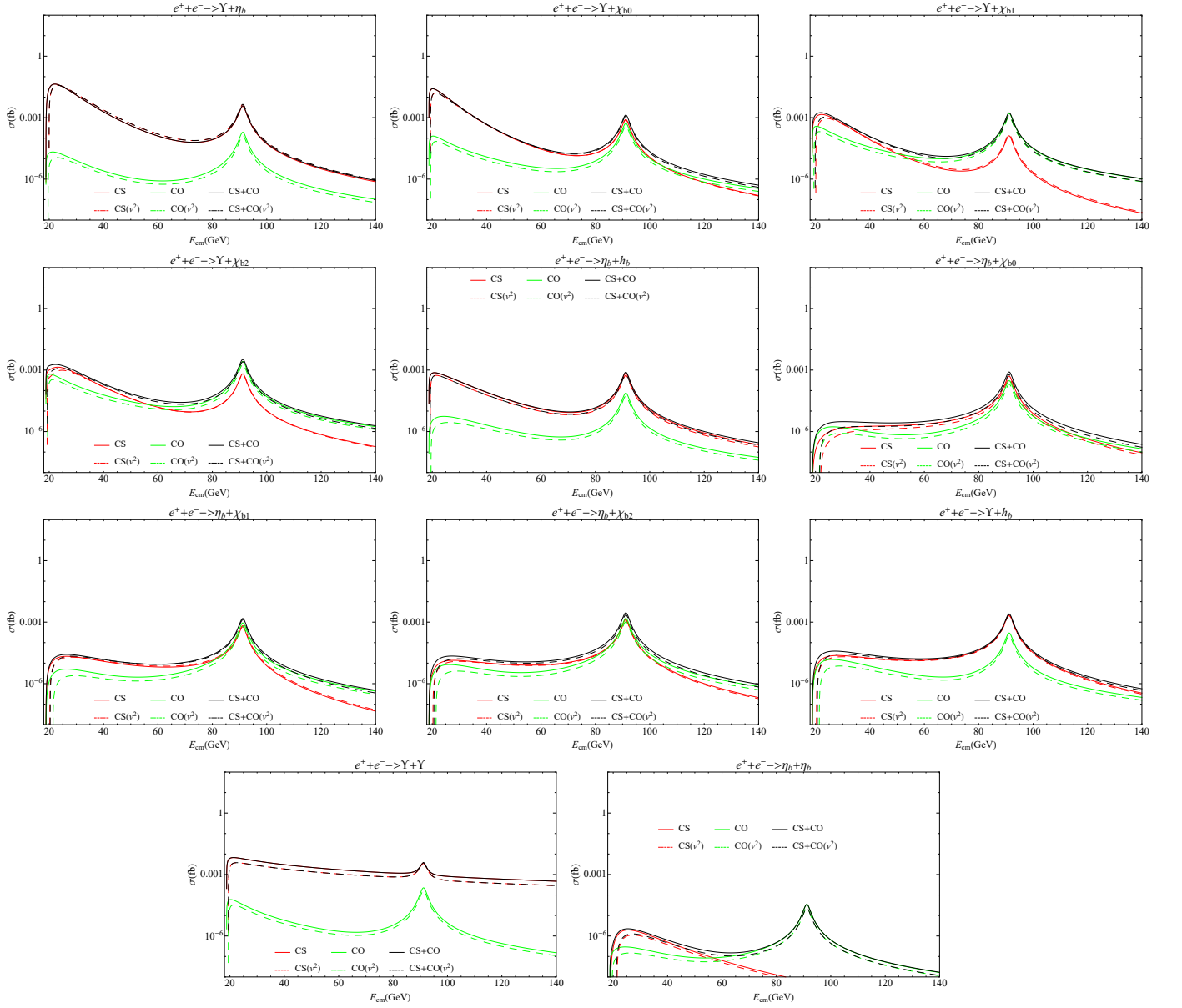


FIG. 3: (Color online) Cross sections ( $\sigma$ ) versus c.m. energy ( $E_{cm} = \sqrt{s}$ ) for double bottomonium production. The solid line represents leading order (LO) and the dashed line represents next-to-leading order in  $v^2$  (NLO) results. The red line represents the CS channel, the green line represents the total CO channels and the black line represents the sum of CS and CO.

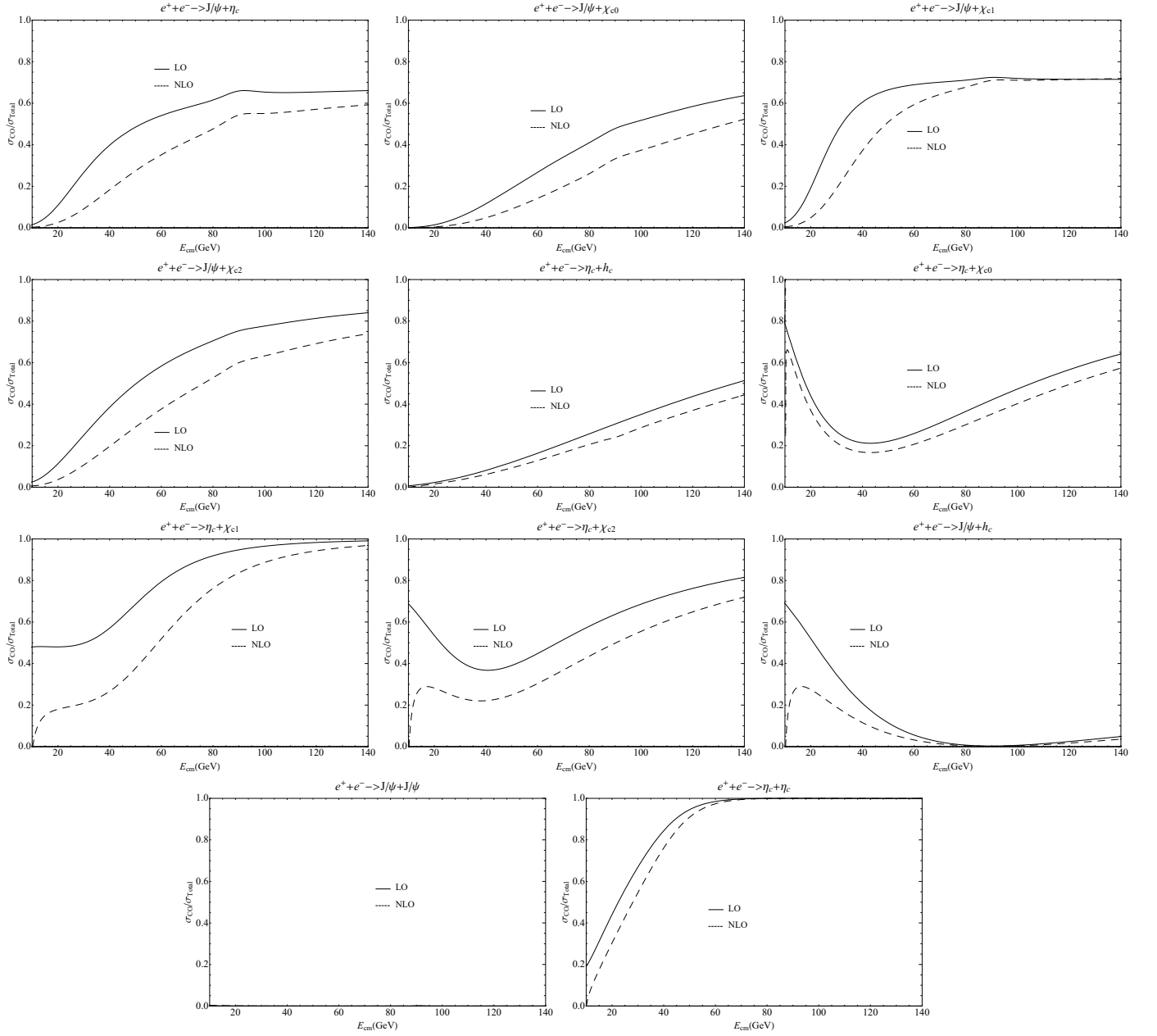


FIG. 4: (Color online) The ratios ( $\sigma_{CO}/\sigma_{Total}$ ) versus c.m. energy ( $E_{cm} = \sqrt{s}$ ) for double charmonium production. The solid line represents leading order (LO) and the dashed line represents next-to-leading order in  $v^2$  (NLO) results.

## B. Events

CEPC has two interaction points. And for its Z factory mode, the designed integrated luminosity within two years is  $16ab^{-1}$ [28]. The FCC-ee, with a designed luminosity of  $150ab^{-1}$ [29], would operate as a super Z factory in its first four years. The designed luminosity of FCC-ee is nine times that of CEPC. The estimated events for CEPC and FCC-ee are shown in Table III.

We use the  $K$  factors of the NLO cross sections for QCD and EW channels in  $\alpha_s$  from Ref. [40] ( $K_{QCD}^{(\alpha_s)} \simeq 3.75, 3.9, 2.55, 2.5$ ,  $K_{EW}^{(\alpha_s)} \simeq 1.08, 1.01, 0.775, 0.908$  for  $J/\psi + \eta_c$ ,  $J/\psi + J/\psi$ ,  $\Upsilon + \eta_b$ ,  $\Upsilon + \Upsilon$ ). Respectively, the NLO( $\alpha_s$ )

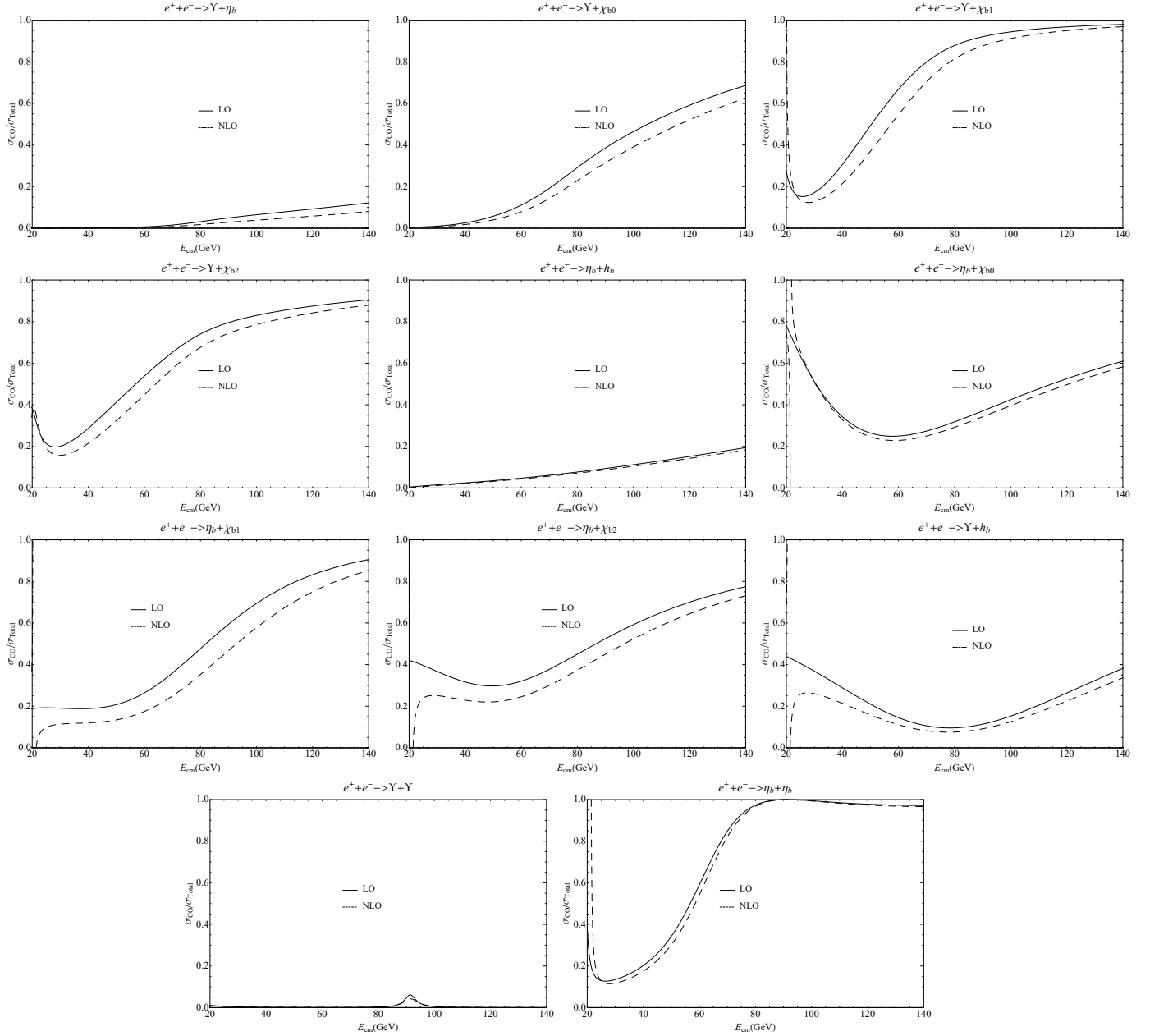


FIG. 5: (Color online) The ratios ( $\sigma_{CO}/\sigma_{Total}$ ) versus c.m. energy ( $E_{cm} = \sqrt{s}$ ) for double bottomonium production. The solid line represents leading order (LO) and the dashed line represents next-to-leading order in  $v^2$  (NLO) results.

cross sections would be obtained as  $\sigma_{CS(QCD)}^{(\alpha_s)} = (0.7; 1.3; 58.9; 28.9) \times 10^{-4} fb$ ,  $\sigma_{CS(EW)}^{(\alpha_s)} = (8.7; 54.8; 1.0; 2.4) \times 10^{-4} fb$ <sup>2</sup>, and with the interference contributions between QCD and EW channels as  $(2.5; 8.4; 11.2; 11.1) \times 10^{-4} fb$ . The CO cross sections are  $(20.9; 1.4; 1.9; 2.2) \times 10^{-4} fb$ . The t-channel double-photon-fragmentation QED contributions are  $(0; 2673.0; 0; 9.1) \times 10^{-4} fb$ . Therefore the total cross section at  $\mathcal{O}(v^0)$  would be  $(32.7; 2738.9; 73.1; 53.8) \times 10^{-4} fb$ , and the final events would be  $(52, 4382, 117, 86)$  and  $(491, 41083, 1096, 806)$  for the two colliders.

<sup>2</sup> The cross sections obtained by summing the QCD and EW contributions for  $\Upsilon + \eta_b$ ,  $\Upsilon + \Upsilon$  processes are different from those in Ref.[40]. This is due to the adoption of different parameters, especially  $\alpha_s$  and LDMEs.

TABLE III: The events of double heavy quarkonia production at  $\sqrt{s}=91.1876$  GeV for the CEPC and FCC-ee. In each cell, the values outside/inside the brackets are for leading order and next-to-leading order results in the  $v^2$  expansions, respectively.

CEPC( $16ab^{-1}$ )					
	CS	CS+CO		CS	CS+CO
$J/\psi + J/\psi$	4378(569)	4380(570)	$\Upsilon + \Upsilon$	55(59)	59(61)
$J/\psi + \eta_c$	17(10)	51(22)	$\Upsilon + \eta_b$	57(69)	60(71)
$J/\psi + h_c$	53(32)	53(32)	$\Upsilon + h_b$	36(33)	40(36)
$J/\psi + \chi_{c0}$	3(2)	7(3)	$\Upsilon + \chi_{b0}$	13(13)	21(19)
$J/\psi + \chi_{c1}$	4(1)	13(5)	$\Upsilon + \chi_{b1}$	2(2)	27(21)
$J/\psi + \chi_{c2}$	5(4)	21(9)	$\Upsilon + \chi_{b2}$	11(10)	53(41)
$\eta_c + \eta_c$	0(0)	63(21)	$\eta_b + \eta_b$	0(0)	1(0)
$\eta_c + h_c$	5(2)	7(3)	$\eta_b + h_b$	11(9)	13(10)
$\eta_c + \chi_{c0}$	11(6)	19(9)	$\eta_b + \chi_{b0}$	8(6)	13(9)
$\eta_c + \chi_{c1}$	1(2)	26(11)	$\eta_b + \chi_{b1}$	9(11)	24(21)
$\eta_c + \chi_{c2}$	23(15)	63(30)	$\eta_b + \chi_{b2}$	21(19)	46(36)
FCC-ee( $150ab^{-1}$ )					
$J/\psi + J/\psi$	41041(5335)	41061(5343)	$\Upsilon + \Upsilon$	516(552)	550(576)
$J/\psi + \eta_c$	163(93)	481(206)	$\Upsilon + \eta_b$	535(645)	564(665)
$J/\psi + h_c$	498(304)	499(304)	$\Upsilon + h_b$	333(305)	378(337)
$J/\psi + \chi_{c0}$	32(21)	61(32)	$\Upsilon + \chi_{b0}$	120(119)	199(176)
$J/\psi + \chi_{c1}$	34(13)	123(45)	$\Upsilon + \chi_{b1}$	20(23)	257(194)
$J/\psi + \chi_{c2}$	48(35)	196(89)	$\Upsilon + \chi_{b2}$	99(95)	494(380)
$\eta_c + \eta_c$	0(0)	587(199)	$\eta_b + \eta_b$	0(0)	5(3)
$\eta_c + h_c$	46(23)	67(31)	$\eta_b + h_b$	106(82)	118(91)
$\eta_c + \chi_{c0}$	102(52)	179(80)	$\eta_b + \chi_{b0}$	75(58)	121(89)
$\eta_c + \chi_{c1}$	12(16)	241(103)	$\eta_b + \chi_{b1}$	88(100)	225(193)
$\eta_c + \chi_{c2}$	211(141)	593(285)	$\eta_b + \chi_{b2}$	200(182)	428(336)

### C. Uncertainties

The sources of uncertainty include the heavy quark mass, LDMEs, renormalization scale, and the deviation of collision energy from  $m_Z$ . As in Ref. [46] and for simplicity, we won't discuss the LDMEs uncertainty. However, the CO LDMEs used in the present paper are actually moderate compared to those in some other Refs. [5, 7, 8, 75–84]. Ref. [43] used five CS LDMEs to see the uncertainties caused by them. When we used the largest set (B.T potential model)[66, 68], we found that the COM is still significant around the  $Z^0$  pole for many processes.

The uncertainties caused by the renormalization scale ( $\mu$ ) are shown in Figs. 11 and 12.

To show the sensitivity of the total cross sections to the collision energy around the  $Z^0$  peak, we calculate the total cross sections using  $E_{cm} = (1 \pm 3\%)m_Z$ . The results are given in Tables IV and V, where we use the same ratios as in Ref. [46].

$$\begin{aligned}
 R_- &= \frac{\sigma(E_{cm} = 97\%m_Z)}{\sigma(E_{cm} = m_Z)} \\
 R_+ &= \frac{\sigma(E_{cm} = 103\%m_Z)}{\sigma(E_{cm} = m_Z)}
 \end{aligned} \tag{33}$$

The total cross section decreases to 15%  $\sim$  20% of its peak values, consistent with the results in Tables VIII and IX of Ref. [46], which studied the semi-exclusive processes.

Next, to see the uncertainty caused by the heavy quark mass, we take  $m_c = (1.5 \pm 0.15) \text{ GeV}$ ,  $m_b = (4.7 \pm 0.15) \text{ GeV}$ . The results are shown in Tables VI and VII. For the charmonium production, the uncertainties associated with the  $m_c = 1.5 \pm 0.15 \text{ GeV}$  variation are as follows.

(i) For the CS channel, the uncertainties are about 0.2% for  $\eta_c + \chi_{c1}$  production, about 16 – 27% for  $J/\psi + h_c/\chi_{c0}/\chi_{c2}$ ,  $\eta_c + h_c/\chi_{c0}/\chi_{c2}/\eta_c$  production, about 24 – 37% for  $J/\psi + \eta_c$  production, about 28 – 45% for  $J/\psi + \chi_{c1}$  production, about 44 – 91% for double  $J/\psi$  production;

(ii) For total CO channels, about 30 – 50% for  $J/\psi + h_c/J/\psi$  production, about 32 – 53% for all other production processes;

(iii) For total cross sections, it's about 18 – 26% for  $J/\psi + h_c$  production, about 21 – 32% for  $J/\psi + \chi_{c0}$ ,  $\eta_c + h_c$

production, about 23 – 38% for  $\eta_c + \chi_{c0}/\chi_{c2}$  production, about 27 – 46% for  $J/\psi + \eta_c/\chi_{c2}, \eta_c + \chi_{c1}$  production, about 31 – 53% for  $J/\psi + \chi_{c1}, \eta_c + \eta_c$  production, about 44 – 91% for double  $J/\psi$  production.

As for the bottomonium production, the uncertainties associated with the variation  $m_b = 4.7 \pm 0.15 \text{ GeV}$  are as follows.

- (i) For the CS channel, the uncertainties are 1% for  $\Upsilon/\eta_b + \chi_{b1}$  production, about 2 – 3% for  $\Upsilon + \eta_b/\chi_{b0}$  production, about 5 – 6% for  $\Upsilon + \chi_{b2}/h_b, \eta_b + \chi_{b2}$  production, about 6 – 8% for  $\eta_b + h_b/\chi_{b0}/\eta_b, \Upsilon + \Upsilon$  production;
- (ii) For total CO channels, it's about 12 – 15% for all production processes;
- (iii) For total cross sections, it's about 3% for  $\Upsilon + \eta_b$  production, about 6% for  $\Upsilon + h_b/\chi_{b0}$  production, about 6 – 8% for  $\eta_b + h_b/\chi_{b1}, \Upsilon + \Upsilon$  production, about 9 – 10% for  $\eta_b + \chi_{b0}/\chi_{b2}$  production, about 11 – 13% for  $\Upsilon + \chi_{b1}/\chi_{b2}$  production, about 13 – 15% for double  $\eta_b$  production.

#### D. $J/\psi + \eta_c$ production

We present cross-sections of  $J/\psi + \eta_c$  production at NLO( $\alpha_s, v^2$ ) with uncertainties induced by the quark mass in the left panel of Fig. 6. From the figure, one can find the effects of CO channels are significant. CS cross sections are summed by those of QCD, EW channels. The  $K$  factors of NLO( $\alpha_s$ ) are estimated from the calculations of Ref.[40], i.e.,  $K_{QCD} = 1.21 - 0.37 \ln(4m_c^2/s)$ , and  $K_{QED} = 0.67 - 0.06 \ln(4m_c^2/s)$ . The central lines correspond to  $m_c = 1.5 \text{ GeV}$ . The upper/lower bounds of the bands correspond to  $m_c = 1.35, 1.65 \text{ GeV}$ , respectively. Furthermore, in an attempt to eliminate the uncertainties associated with CS LDMEs, we plot the ratios of the production rates of  $J/\psi + \eta_c$  to those of double  $J/\psi$  in the right panel.

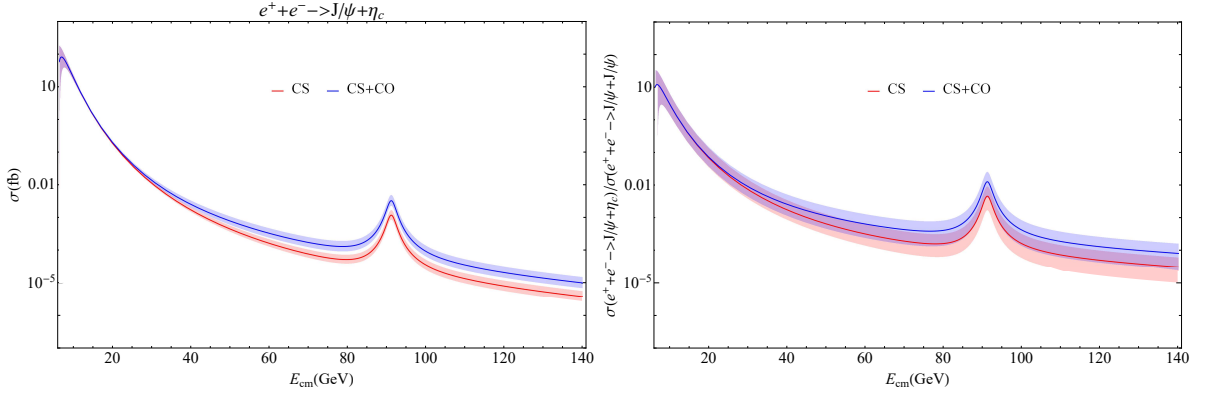


FIG. 6: (Color online) The cross sections with uncertainties of  $J/\psi + \eta_c$  production (left panel). The ratios between the cross sections of  $J/\psi + \eta_c$  production and that of double  $J/\psi$  production (right panel).

#### V. SUMMARY

In this paper, we have studied the production of double heavy quarkonium in  $e^+e^-$  annihilation at the Z factories, considering the CO contributions along with CS channels up-to  $\mathcal{O}(v^2)$ .

We considered CS channels including QCD and EW processes and all the CO channels at the level of tree diagrams in the calculations. The CO channels contribute substantially more than the CS channels in several processes, particularly for the combinations involving the  $^3S_1^{[8]}$  state. This indicates that the processes of gluon fragmentation into the intermediate  $^3S_1^{[8]}$  state might play a crucial role. It implies that studying the production of double heavy quarkonia may also be a good way to determine the LDMEs  $\langle \mathcal{O}^H(^3S_1^{[8]}) \rangle$  in the future Z factory experiment with precise measurement. Meanwhile, the relativistic corrections are significant and the LO cross sections would be suppressed by the factors of at least 50% for charmonia and 20% for bottomonia, respectively. With the results of cross sections, we estimate the events of double heavy quarkonium production for future experimental measurements (CEPC and FCC-ee).

The COM is indispensable in hadron collision processes[5, 7, 8, 79, 82, 84], while in the double charmonium production via  $e^+e^-$  annihilation at B factory, the COM is negligible[85]. In this work, we show that the COM is



significant or dominant in  $e^+e^-$  annihilation at Z factory and higher collision energy. It is expected that the COM is also significant for some other heavy quarkonia production processes (e.g. inclusive production processes, or D-wave heavy quarkonia production) at the Z factory and higher energy region. However, the COM may be negligible for  $B_c$  meson production, since the gluon can't be fragmented into a  $3S_1^{[8]} c\bar{c}$  quark pair. And it will be important to continue to calculate QCD loop corrections to these processes to complement the study of heavy quarkonia production at future  $e^+e^-$  colliders.

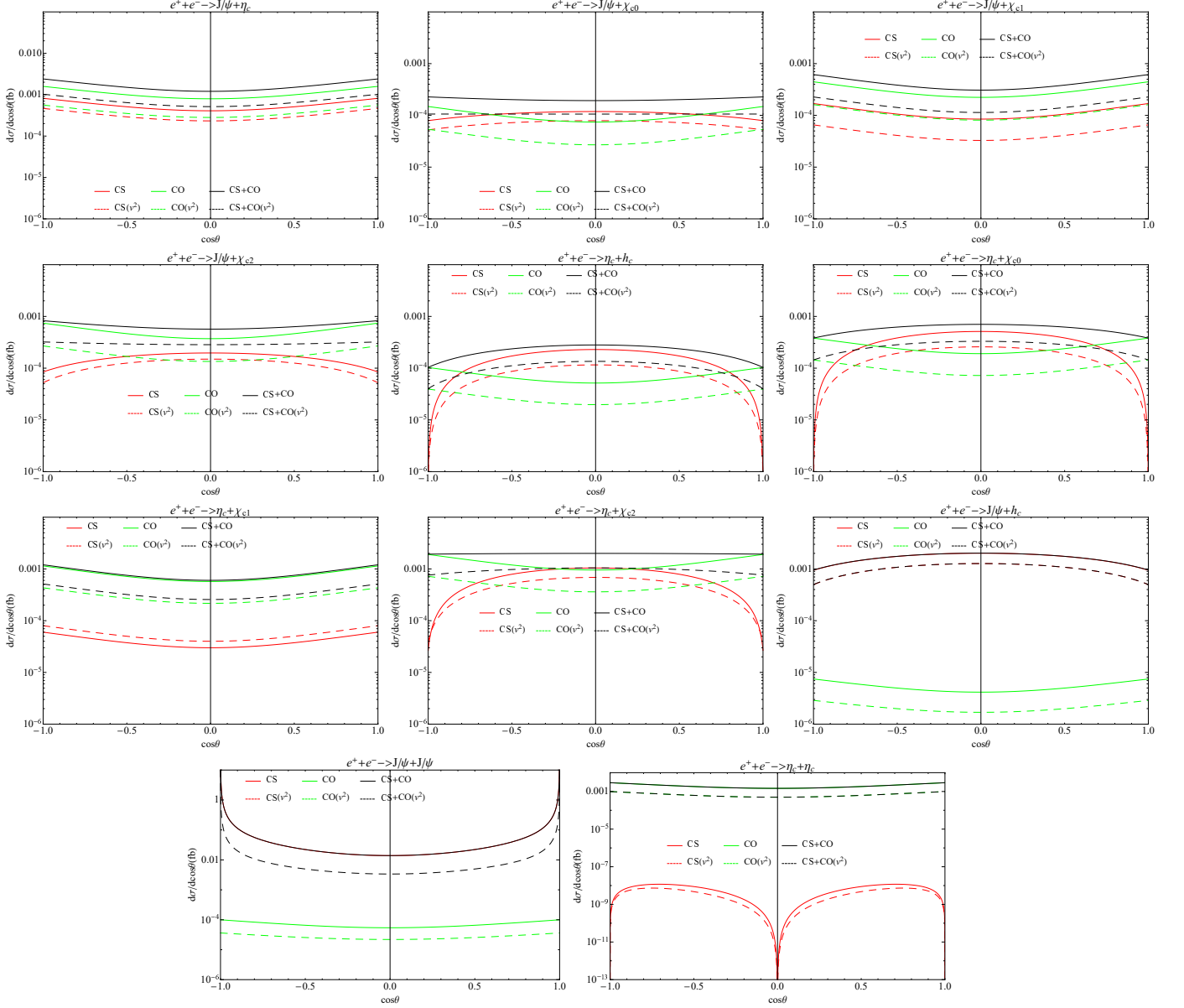


FIG. 7: (Color online) The differential cross sections  $d\sigma/d\cos\theta$  for double charmonium production at  $\sqrt{s}=m_Z$ . The solid line represents leading order (LO) and the dashed line represents next-to-leading order in  $v^2$  (NLO) results. The red line represents the CS channel, the green line represents the total CO channels and the black line represents the sum of CS and CO.

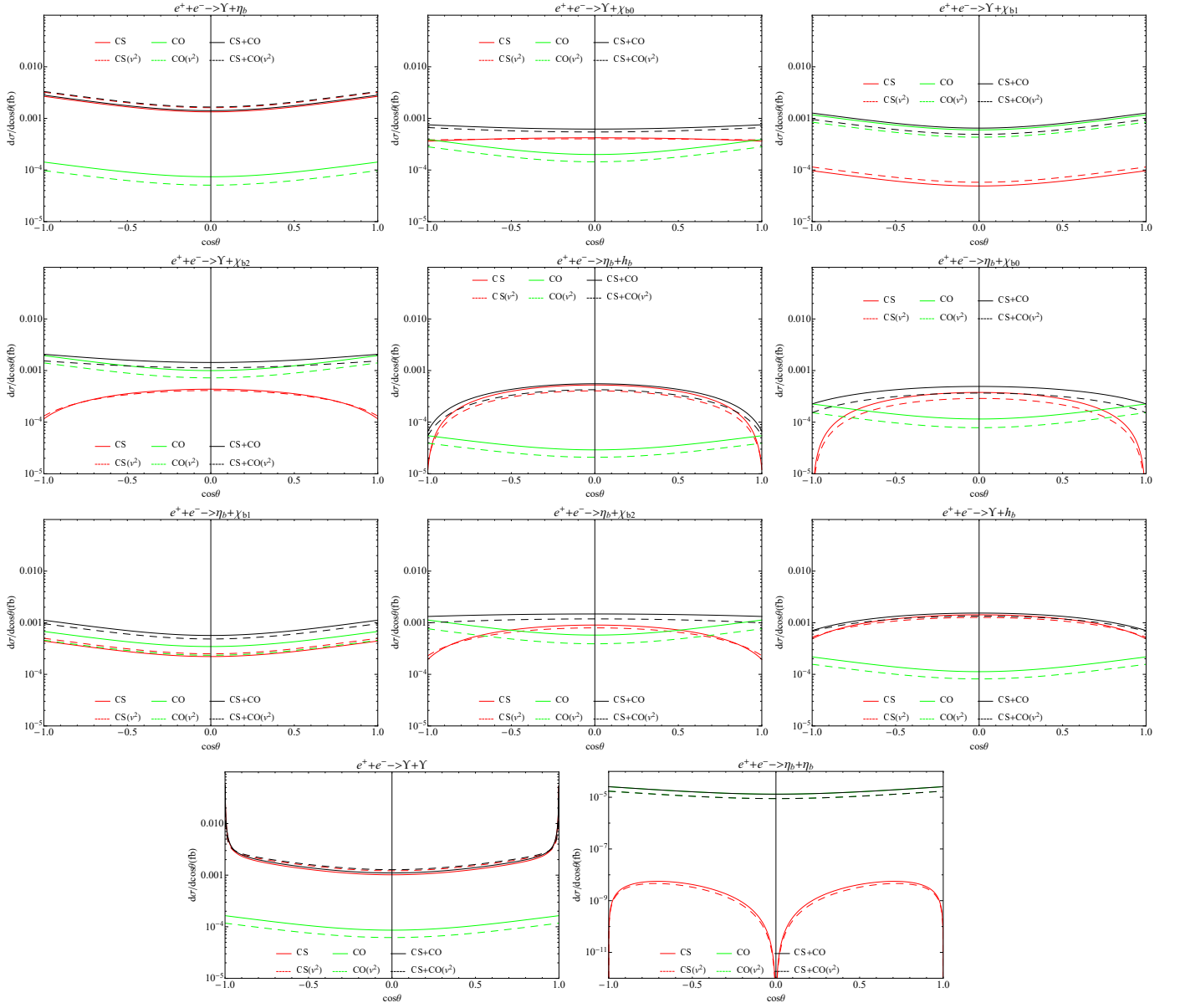


FIG. 8: (Color online) The differential cross sections  $d\sigma/d\cos\theta$  for double bottomonium production at  $\sqrt{s}=m_Z$ .

The solid line represents leading order (LO) and the dashed line represents next-to-leading order in  $v^2$  (NLO) results. The red line represents the CS channel, the green line represents the total CO channels and the black line represents the sum of CS and CO.

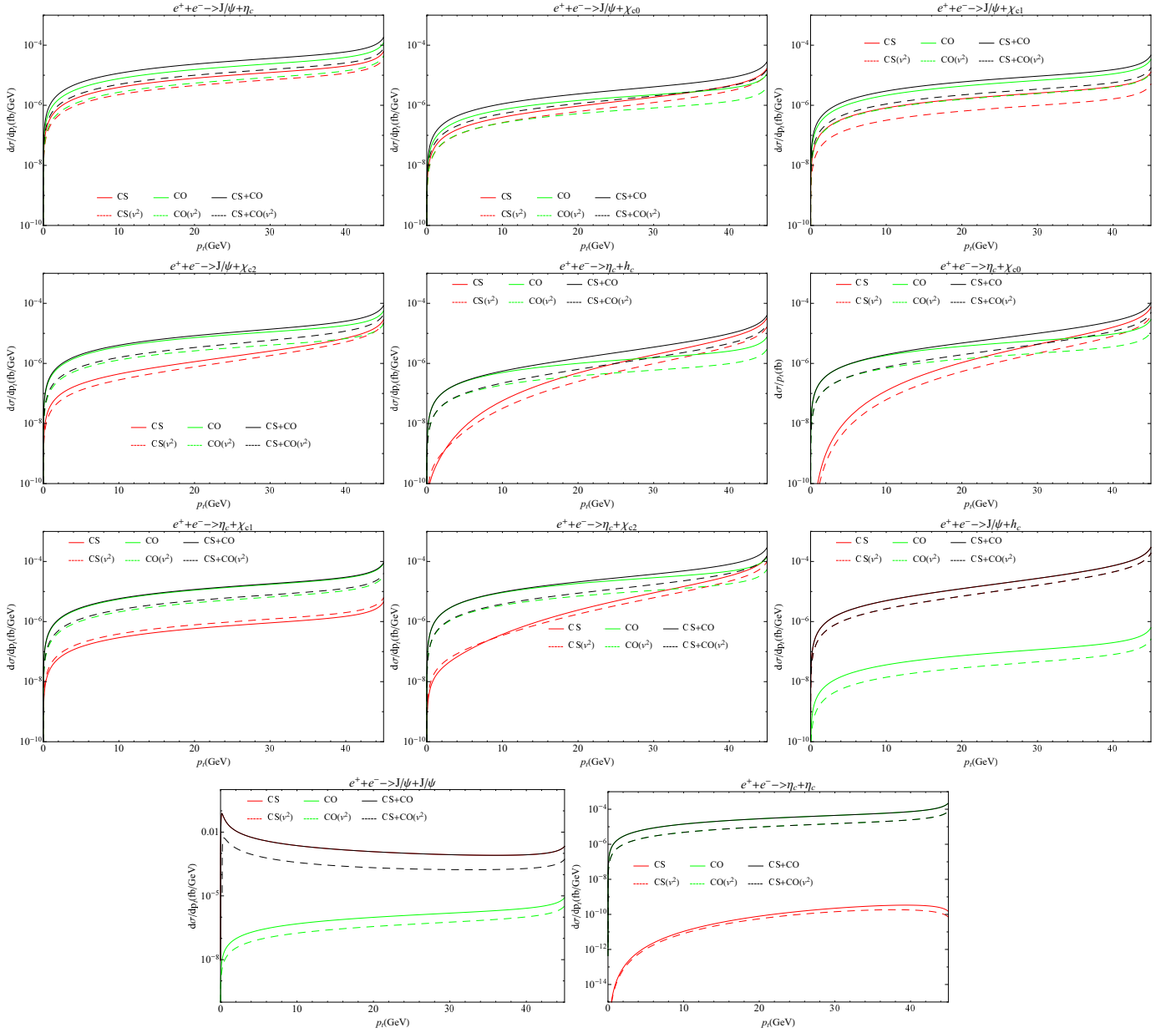


FIG. 9: (Color online) The differential cross sections ( $d\sigma/dp_t$ ) for double charmonium production at  $\sqrt{s}=m_Z$ . The solid line represents leading order (LO) and the dashed line represents next-to-leading order in  $v^2$  (NLO) results. The red line represents the CS channel, the green line represents the total CO channels and the black line represents the sum of CS and CO.

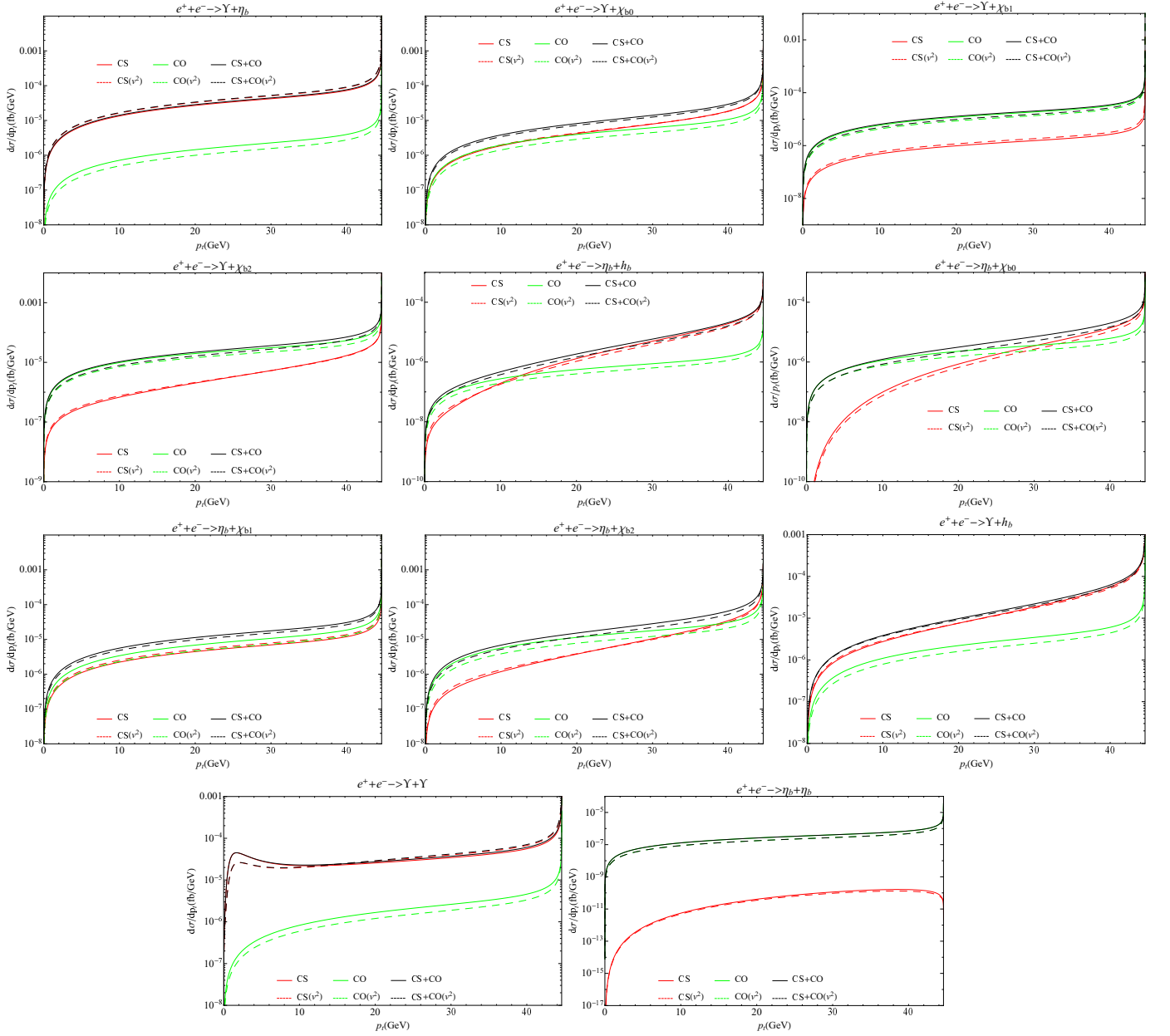


FIG. 10: (Color online) The differential cross section ( $d\sigma/dp_t$ ) for double bottomonium production at  $\sqrt{s}=m_Z$ . The solid line represents leading order (LO) and the dashed line represents next-to-leading order in  $v^2$  (NLO) results. The red line represents the CS channel, the green line represents the total CO channels and the black line represents the sum of CS and CO.

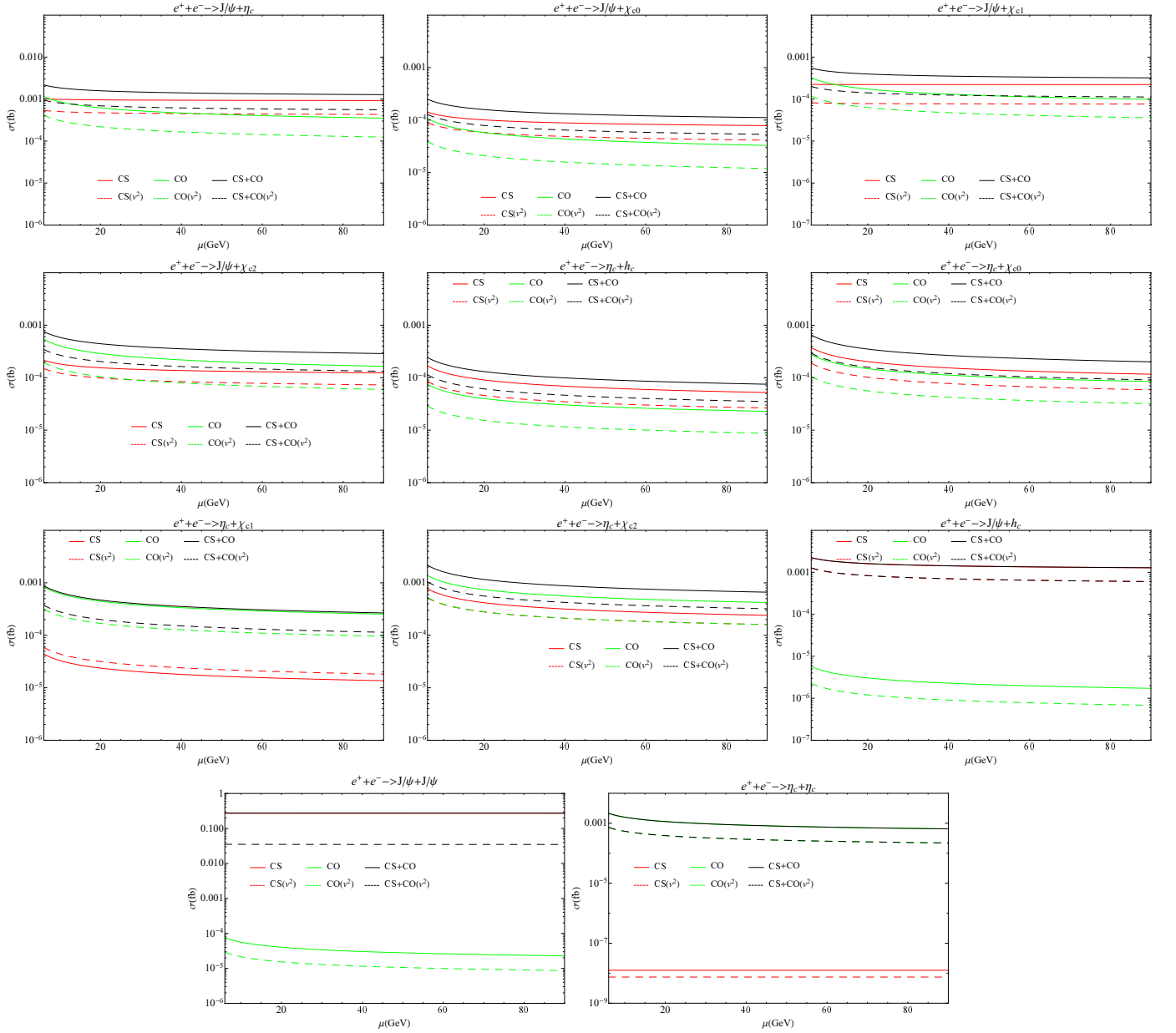


FIG. 11: (Color online) Cross sections ( $\sigma$ ) versus renormalization scale ( $\mu$ ) for double charmonium production at  $\sqrt{s}=m_Z$ . The solid line represents LO and dashed line represents NLO( $v^2$ ) result. The solid line represents leading order (LO) and the dashed line represents next-to-leading order in  $v^2$  (NLO) results. The red line represents the CS channel, the green line represents the total CO channels and the black line represents the sum of CS and CO.

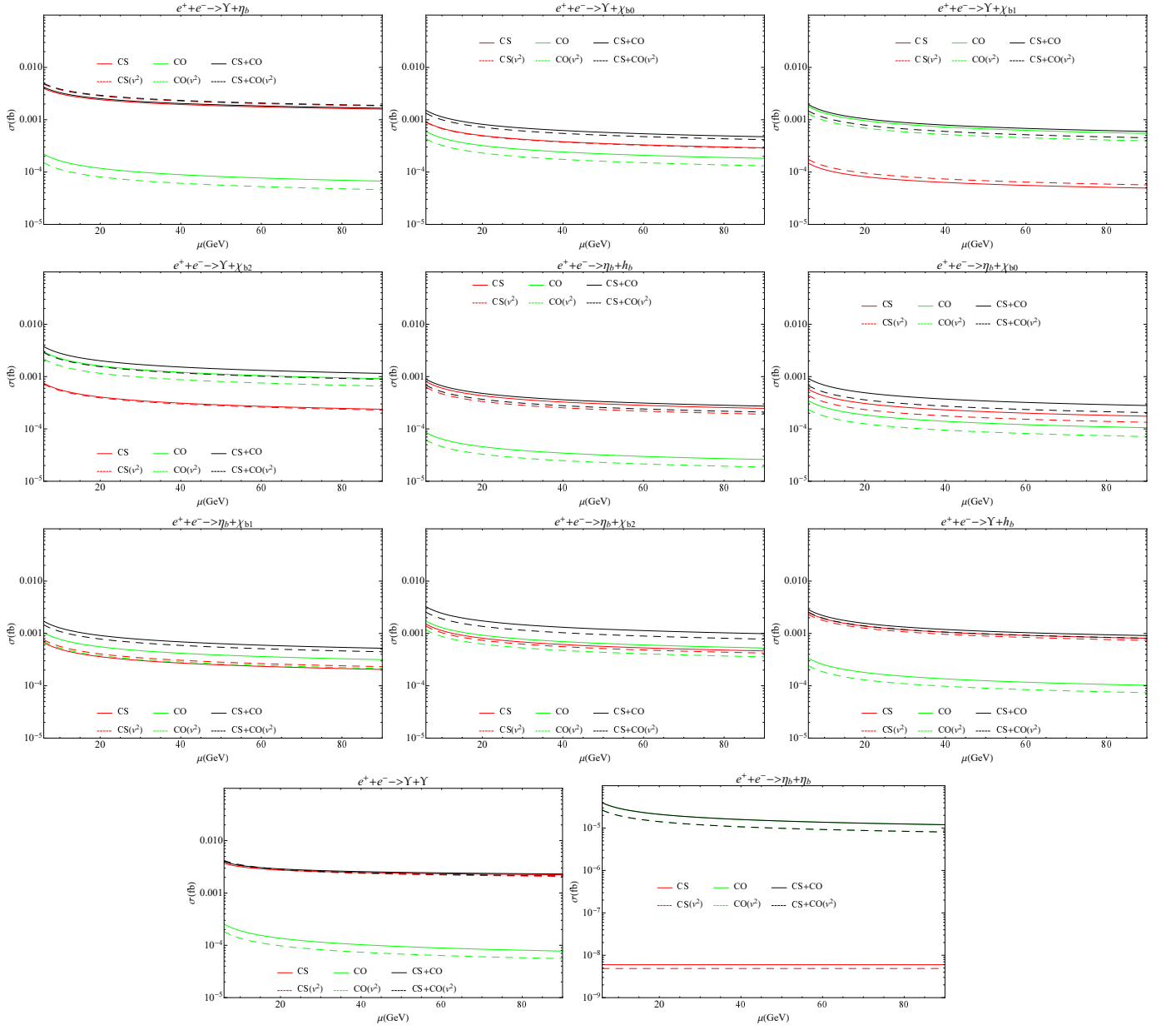


FIG. 12: (Color online) Cross section ( $\sigma$ ) versus renormalization scale ( $\mu$ ) for double bottomonium production at  $\sqrt{s}=m_Z$ . The solid line represents leading order (LO) and the dashed line represents next-to-leading order in  $v^2$  (NLO) results. The red line represents the CS channel, the green line represents the total CO channels and the black line represents the sum of CS and CO.

TABLE IV: Total cross sections (*units* :  $\times 10^{-4}$  fb) up to  $\mathcal{O}(v^2)$  for the double charmonia production, with varying values of  $E_{cm}$ . The ratio  $R_{\pm}$  show how the cross sections are changed with varying  $E_{cm}$ .

	CS			CO			Total		
	97% $m_Z$	103% $m_Z$	$\begin{pmatrix} R_- \\ R_+ \end{pmatrix}$	97% $m_Z$	103% $m_Z$	$\begin{pmatrix} R_- \\ R_+ \end{pmatrix}$	97% $m_Z$	103% $m_Z$	$\begin{pmatrix} R_- \\ R_+ \end{pmatrix}$
$J/\psi + \eta_c$	1.2	1.1	$\begin{pmatrix} 19\% \\ 18\% \end{pmatrix}$	1.4	1.4	$\begin{pmatrix} 18\% \\ 18\% \end{pmatrix}$	2.6	2.5	$\begin{pmatrix} 19\% \\ 18\% \end{pmatrix}$
$J/\psi + h_c$	3.8	3.2	$\begin{pmatrix} 19\% \\ 16\% \end{pmatrix}$	0.0	0.0	$\begin{pmatrix} 19\% \\ 19\% \end{pmatrix}$	3.8	3.2	$\begin{pmatrix} 19\% \\ 16\% \end{pmatrix}$
$J/\psi + \chi_{c0}$	0.3	0.2	$\begin{pmatrix} 20\% \\ 18\% \end{pmatrix}$	0.1	0.1	$\begin{pmatrix} 18\% \\ 19\% \end{pmatrix}$	0.4	0.4	$\begin{pmatrix} 19\% \\ 18\% \end{pmatrix}$
$J/\psi + \chi_{c1}$	0.2	0.2	$\begin{pmatrix} 19\% \\ 19\% \end{pmatrix}$	0.4	0.4	$\begin{pmatrix} 18\% \\ 19\% \end{pmatrix}$	0.6	0.6	$\begin{pmatrix} 19\% \\ 19\% \end{pmatrix}$
$J/\psi + \chi_{c2}$	0.5	0.4	$\begin{pmatrix} 20\% \\ 18\% \end{pmatrix}$	0.7	0.7	$\begin{pmatrix} 18\% \\ 19\% \end{pmatrix}$	1.1	1.1	$\begin{pmatrix} 19\% \\ 18\% \end{pmatrix}$
$\eta_c + h_c$	0.3	0.3	$\begin{pmatrix} 20\% \\ 18\% \end{pmatrix}$	0.1	0.1	$\begin{pmatrix} 19\% \\ 19\% \end{pmatrix}$	0.4	0.4	$\begin{pmatrix} 19\% \\ 18\% \end{pmatrix}$
$\eta_c + \chi_{c0}$	0.6	0.5	$\begin{pmatrix} 19\% \\ 16\% \end{pmatrix}$	0.3	0.3	$\begin{pmatrix} 18\% \\ 17\% \end{pmatrix}$	1.0	0.9	$\begin{pmatrix} 18\% \\ 16\% \end{pmatrix}$
$\eta_c + \chi_{c1}$	0.2	0.2	$\begin{pmatrix} 20\% \\ 15\% \end{pmatrix}$	1.0	1.0	$\begin{pmatrix} 18\% \\ 17\% \end{pmatrix}$	1.2	1.1	$\begin{pmatrix} 18\% \\ 17\% \end{pmatrix}$
$\eta_c + \chi_{c2}$	1.8	1.5	$\begin{pmatrix} 19\% \\ 16\% \end{pmatrix}$	1.7	1.6	$\begin{pmatrix} 18\% \\ 17\% \end{pmatrix}$	3.5	3.1	$\begin{pmatrix} 18\% \\ 16\% \end{pmatrix}$
$J/\psi + J/\psi$	669.4	620.0	$\begin{pmatrix} 94\% \\ 87\% \end{pmatrix}$	0.2	0.2	$\begin{pmatrix} 19\% \\ 18\% \end{pmatrix}$	670.0	620.0	$\begin{pmatrix} 94\% \\ 87\% \end{pmatrix}$
$\eta_c + \eta_c$	0.0	0.0	$\begin{pmatrix} 120\% \\ 84\% \end{pmatrix}$	4.7	4.5	$\begin{pmatrix} 18\% \\ 17\% \end{pmatrix}$	4.7	4.5	$\begin{pmatrix} 18\% \\ 17\% \end{pmatrix}$



TABLE V: Total cross sections (*units* :  $\times 10^{-4} fb$ ) up to  $\mathcal{O}(v^2)$  for the double bottomonia production, with varying values of  $E_{cm}$ . The ratio  $R_{\pm}$  show how the cross sections are changed with varying  $E_{cm}$ .

	CS			CO			Total		
	97% $m_Z$	103% $m_Z$	$\left(\frac{R_-}{R_+}\right)$	97% $m_Z$	103% $m_Z$	$\left(\frac{R_-}{R_+}\right)$	97% $m_Z$	103% $m_Z$	$\left(\frac{R_-}{R_+}\right)$
$\Upsilon + \eta_b$	8.3	6.7	$\left(\frac{19\%}{16\%}\right)$	0.2	0.2	$\left(\frac{17\%}{17\%}\right)$	8.6	6.9	$\left(\frac{19\%}{16\%}\right)$
$\Upsilon + h_b$	3.9	3.2	$\left(\frac{19\%}{16\%}\right)$	0.4	0.4	$\left(\frac{17\%}{17\%}\right)$	4.2	3.6	$\left(\frac{19\%}{16\%}\right)$
$\Upsilon + \chi_{b0}$	1.5	1.2	$\left(\frac{19\%}{16\%}\right)$	0.7	0.7	$\left(\frac{17\%}{17\%}\right)$	2.2	1.9	$\left(\frac{19\%}{16\%}\right)$
$\Upsilon + \chi_{b1}$	0.3	0.2	$\left(\frac{20\%}{15\%}\right)$	2.0	2.0	$\left(\frac{17\%}{17\%}\right)$	2.3	2.2	$\left(\frac{18\%}{17\%}\right)$
$\Upsilon + \chi_{b2}$	1.2	1.0	$\left(\frac{19\%}{16\%}\right)$	3.3	3.3	$\left(\frac{17\%}{17\%}\right)$	4.5	4.3	$\left(\frac{18\%}{17\%}\right)$
$\eta_b + h_b$	1.0	0.9	$\left(\frac{18\%}{16\%}\right)$	0.1	0.1	$\left(\frac{17\%}{17\%}\right)$	1.1	1.0	$\left(\frac{18\%}{16\%}\right)$
$\eta_b + \chi_{b0}$	0.7	0.6	$\left(\frac{19\%}{16\%}\right)$	0.4	0.4	$\left(\frac{17\%}{17\%}\right)$	1.1	1.0	$\left(\frac{18\%}{16\%}\right)$
$\eta_b + \chi_{b1}$	1.3	1.0	$\left(\frac{20\%}{15\%}\right)$	1.1	1.1	$\left(\frac{17\%}{17\%}\right)$	2.4	2.1	$\left(\frac{19\%}{16\%}\right)$
$\eta_b + \chi_{b2}$	2.3	1.9	$\left(\frac{19\%}{16\%}\right)$	1.8	1.8	$\left(\frac{17\%}{17\%}\right)$	4.1	3.7	$\left(\frac{18\%}{16\%}\right)$
$\Upsilon + \Upsilon$	12.5	9.6	$\left(\frac{34\%}{26\%}\right)$	0.3	0.3	$\left(\frac{18\%}{17\%}\right)$	12.8	9.9	$\left(\frac{18\%}{17\%}\right)$
$\eta_b + \eta_b$	0.0	0.0	$\left(\frac{119\%}{84\%}\right)$	0.0	0.0	$\left(\frac{17\%}{17\%}\right)$	0.0	0.0	$\left(\frac{17\%}{17\%}\right)$

TABLE VI: Total cross sections (*units* :  $\times 10^{-4} fb$ ) up to  $\mathcal{O}(v^2)$  for the double charmonia production at  $\sqrt{s} = m_Z$ , with varying values of  $m_c$ . The uncertainties in each the third column are the deviations from the central values corresponding to  $m_c = 1.5 GeV$ .

$m_c$	CS			CO			Total		
	1.35GeV	1.65GeV	uncertainty	1.35GeV	1.65GeV	uncertainty	1.35GeV	1.65GeV	uncertainty
$J/\psi + \eta_c$	8.510	4.732	+2.300 -1.477	11.47	5.102	+3.971 -2.397	19.98	9.835	+6.271 -3.874
$J/\psi + h_c$	25.41	16.57	+5.167 -3.677	0.063	0.029	+0.021 -0.013	25.48	16.60	+5.188 -3.690
$J/\psi + \chi_{c0}$	1.707	1.184	+0.305 -0.218	1.099	0.489	+0.380 -0.230	2.806	1.673	+0.685 -0.448
$J/\psi + \chi_{c1}$	1.271	0.631	+0.397 -0.243	3.296	1.467	+1.141 -0.689	4.566	2.098	+1.537 -0.931
$J/\psi + \chi_{c2}$	2.967	1.902	+0.624 -0.440	5.493	2.444	+1.901 -1.148	8.460	4.347	+2.525 -1.588
$\eta_c + h_c$	1.916	1.275	+0.368 -0.273	0.805	0.358	+0.279 -0.168	2.721	1.633	+0.647 -0.441
$\eta_c + \chi_{c0}$	4.268	2.833	+0.825 -0.610	2.947	1.306	+1.024 -0.617	7.215	4.139	+1.848 -1.227
$\eta_c + \chi_{c1}$	1.069	1.064	+0.002 -0.003	8.840	3.918	+3.071 -1.852	9.909	4.982	+3.073 -1.855
$\eta_c + \chi_{c2}$	11.51	7.860	+2.097 -1.552	14.73	6.529	+5.118 -3.087	26.24	14.39	+7.216 -4.639
$J/\psi + J/\psi$	679.0	199.8	+323.3 -155.9	0.796	0.375	+0.262 -0.160	679.8	200.2	+323.6 -156.0
$\eta_c + \eta_c$	0.000	0.000	+0.000 -0.000	20.35	9.005	+7.076 -4.266	20.35	9.006	+7.076 -4.266

TABLE VII: Total cross sections (*units* :  $\times 10^{-4} fb$ ) up to  $\mathcal{O}(v^2)$  for the double bottomonia production at  $\sqrt{s} = m_Z$ , with varying values of  $m_b$ . The uncertainties in each the third column are the deviations from the central values corresponding to  $m_b = 4.7 GeV$ .

$m_b$	CS			CO			Total		
	4.55GeV	4.85GeV	uncertainty	4.55GeV	4.85GeV	uncertainty	4.55GeV	4.85GeV	uncertainty
$\Upsilon + \eta_b$	44.12	42.00	+1.105 -1.014	1.526	1.162	+0.197 -0.167	45.64	43.16	+1.302 -1.181
$\Upsilon + h_b$	21.46	19.37	+1.093 -0.998	2.436	1.870	+0.306 -0.260	23.89	21.24	+1.399 -1.257
$\Upsilon + \chi_{b0}$	8.112	7.721	+0.204 -0.187	4.354	3.329	+0.554 -0.471	12.47	11.05	+0.758 -0.658
$\Upsilon + \chi_{b1}$	1.554	1.516	+0.020 -0.019	13.06	9.987	+1.662 -1.412	14.61	11.50	+1.681 -1.430
$\Upsilon + \chi_{b2}$	6.716	6.021	+0.364 -0.332	21.77	16.65	+2.770 -2.353	28.48	22.67	+3.134 -2.684
$\eta_b + h_b$	5.915	5.112	+0.421 -0.382	0.618	0.473	+0.078 -0.066	6.532	5.586	+0.499 -0.448
$\eta_b + \chi_{b0}$	4.138	3.577	+0.294 -0.267	2.372	1.795	+0.312 -0.265	6.510	5.373	+0.606 -0.531
$\eta_b + \chi_{b1}$	6.707	6.620	+0.043 -0.044	7.115	5.385	+0.937 -0.794	13.82	12.01	+0.980 -0.838
$\eta_b + \chi_{b2}$	12.78	11.53	+0.658 -0.601	11.86	8.975	+1.561 -1.323	24.64	20.50	+2.219 -1.923
$\Upsilon + \Upsilon$	39.49	34.55	+2.671 -2.266	1.835	1.413	+0.228 -0.194	41.32	35.96	+2.899 -2.459
$\eta_b + \eta_b$	0.000	0.000	+0.000 -0.000	0.268	0.203	+0.035 -0.030	0.268	0.203	+0.035 -0.030

## VI. APPENDIX. A

The ratios of  $\sigma_{NLO(v^2)}/\sigma_{LO}$  (i.e., the  $K$  factors) as a function of  $\sqrt{s}$  are shown as follows.

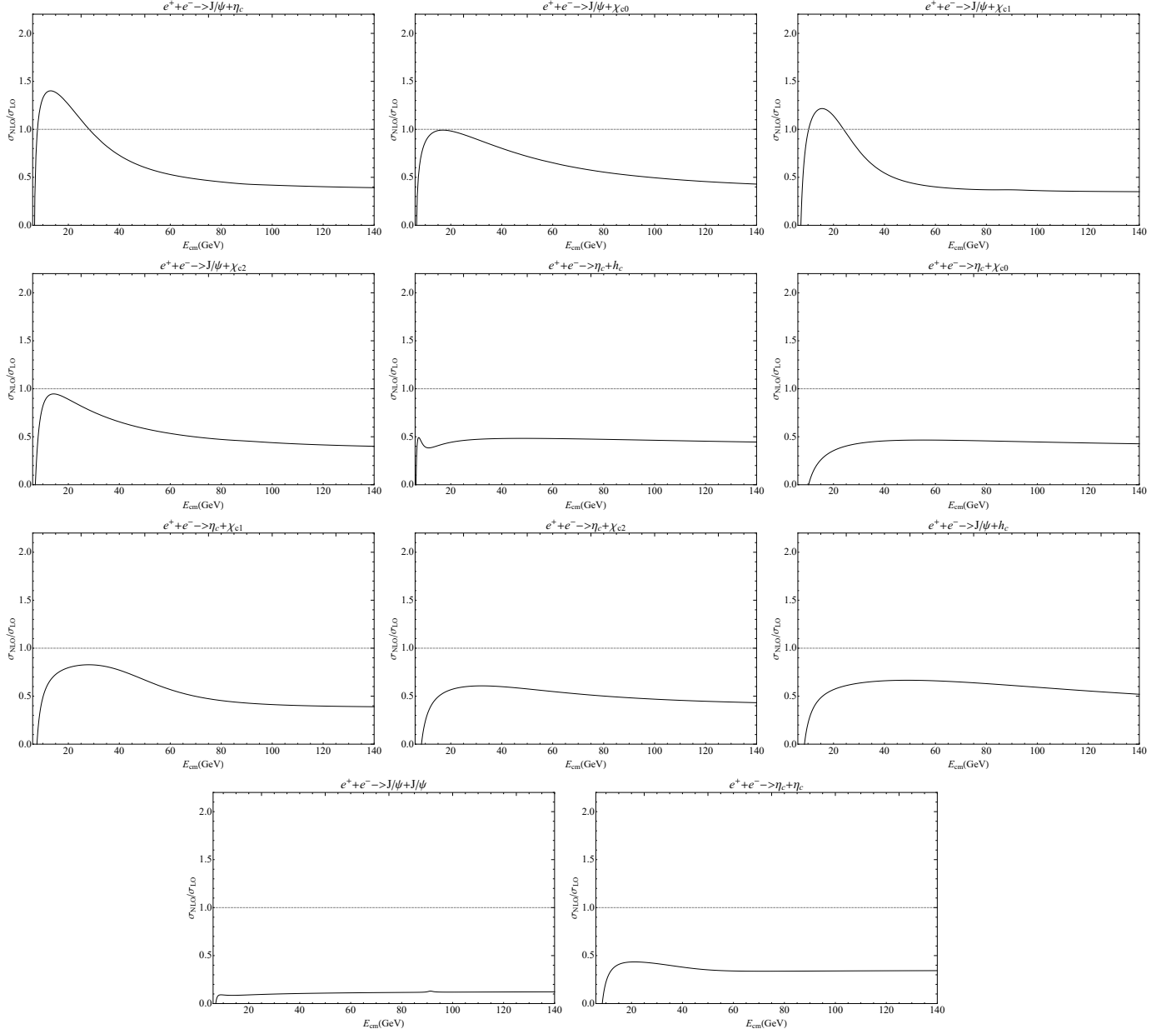


FIG. 13: (Color online) The  $K$  factors for next-to-leading order cross sections in  $v^2$  as a function of c.m. energy for the production of double charmonium.

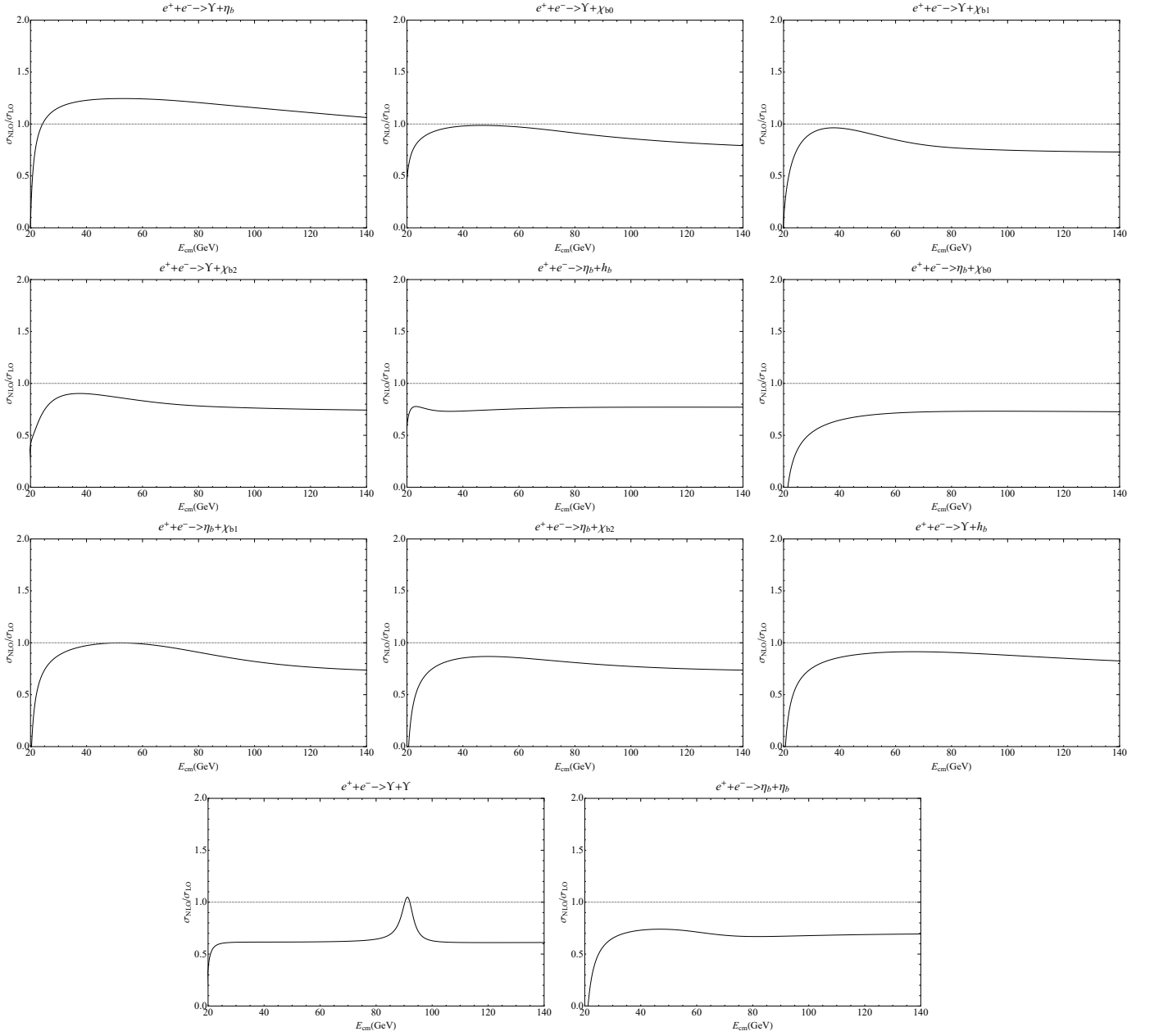


FIG. 14: (Color online) The  $K$  factors for next-to-leading order cross sections in  $v^2$  as a function of c.m. energy for the production of double bottomonium.

## VII. APPENDIX. B

Rather than presenting the analytical expression of the SDCs, we provide in Table VIII the ratios of relativistic correction SDCs (denoted as G) to LO SDCs (denoted as F) in the high c.m. energy limit ( $m_Q^2 \ll s$ ). For specific states, the ratios are determined by the topologies of the Feynman diagrams. Consequently, each ratio is applicable to both charmonia and bottomonia in the channels with consistent states. The gluon fragmentation processes into  $^3S_1^{[8]}$  are dominated for the  $^3S_1^{[8]}$  channels associated with  $^1S_0^{[8]}$ ,  $^3P_J^{[8]}$ ,  $^1P_1^{[8]}$  states. Their ratios can be verified against the Refs.[49, 86]. And the photon fragmentation processes into  $^3S_1^{[1]}$  are dominated for the CS channels of  $J/\psi$  production associated with  $\eta_c$ ,  $\chi_{c0,1,2}$ ,  $h_c$ . Their ratios can be verified against the Refs. [87]. In the high c.m. energy limit, the  $K$  factors for  $NLO(v^2)$  can be obtained from the ratios. In the energy region near  $Z^0$  pole, the  $K$  factors would be jointly determined by the ratios of the non-fragmentation and fragmentation processes for  $J/\psi$  exclusive production.

TABLE VIII: Ratios of relativistic correction SDCs (denoted as G) to LO SDCs (denoted as F) in the high c.m. energy limit ( $m_Q^2 \ll s$ ). In each cell, we define,  $R_i \equiv G[n_i]/F[n_1 + n_2]$ ,  $c = 1, 8$  for CS or CO states and (nf/f) as the non-fragmentation/fragmentation processes corresponding to (a,b,e,f)/(c,d,g,h) diagrams in Fig.1. The first three rows correspond to positive total C-parity of final states and are applicable to  $\gamma^* Z^0$ -propagated processes, while the second group of three rows correspond to negative C-parity and are applicable only to  $Z^0$ -propagated processes. The last rows correspond to the t-channel processes.

$(\text{nf})^3 S_1^{[1,8]} + {}^1 S_0^{[1,8]}$	$R_1 = \frac{3}{2} \quad R_2 = \frac{11}{6}$	$(\text{nf})^3 S_1^{[1,8]} + {}^3 P_0^{[1,8]}$	$R_1 = -\frac{1}{6} \quad R_2 = -\frac{13}{10}$	$(\text{nf})^3 S_1^{[1,8]} + {}^3 P_1^{[1,8]}$	$R_1 = \frac{3}{2} \quad R_2 = \frac{1}{2}$
$(\text{nf})^3 S_1^{[1,8]} + {}^3 P_2^{[1,8]}$	$R_1 = -\frac{1}{6} \quad R_2 = -\frac{7}{10}$	$(\text{nf})^1 S_0^{[1,8]} + {}^1 P_1^{[1,8]}$	$R_1 = -\frac{5}{6} \quad R_2 = -\frac{13}{10}$	$(f)^3 S_1^{[1,8]} + {}^1 S_0^{[1,8]}$	$R_1 = -\frac{11}{6} \quad R_2 = -\frac{5}{6}$
$(f)^3 S_1^{[1,8]} + {}^3 P_0^{[1,8]}$	$R_1 = -\frac{11}{6} \quad R_2 = -\frac{13}{10}$	$(f)^3 S_1^{[1,8]} + {}^3 P_1^{[1,8]}$	$R_1 = -\frac{11}{6} \quad R_2 = -\frac{11}{10}$	$(f)^3 S_1^{[1,8]} + {}^3 P_2^{[1,8]}$	$R_1 = -\frac{11}{6} \quad R_2 = -\frac{7}{10}$
$(f)^3 S_1^{[8]} + {}^3 P_J^{[8]}$	$R_1 = -\frac{11}{6} \quad R_2 = -\frac{31}{30}$	$(\text{nf})^3 P_J^{[8]} + {}^1 P_1^{[8]}$	$R_1 = -\frac{11}{10} \quad R_2 = -\frac{13}{10}$		
$(\text{nf})^3 S_1^{[1,8]} + {}^1 P_1^{[1,8]}$	$R_1 = -\frac{1}{6} \quad R_2 = -\frac{13}{10}$	$(\text{nf})^1 S_0^{[1]} + {}^3 P_0^{[1]}$	$R_1 = -\frac{5}{6} \quad R_2 = -\frac{13}{10}$	$(\text{nf})^1 S_0^{[1]} + {}^3 P_1^{[1]}$	$R_1 = \frac{7}{6} \quad R_2 = \frac{3}{10}$
$(\text{nf})^1 S_0^{[1]} + {}^3 P_2^{[1]}$	$R_1 = -\frac{5}{6} \quad R_2 = -\frac{7}{10}$	$(\text{nf})^1 S_0^{[8]} + {}^3 P_J^{[8]}$	$R_1 = -\frac{5}{6} \quad R_2 = -\frac{9}{10}$	$(f)^3 S_1^{[1,8]} + {}^1 P_1^{[1,8]}$	$R_1 = -\frac{11}{6} \quad R_2 = -\frac{13}{10}$
$(f)^3 S_1^{[8]} + {}^3 S_1^{[8]}$	$R_1 = R_2 = -1$	$(\text{nf})^3 P_J^{[8]} + {}^3 P_J^{[8]}$	$R_1 = R_2 = -1$	$(\text{nf})^1 P_1^{[8]} + {}^1 P_1^{[8]}$	$R_1 = R_2 = \frac{6}{5}$
${}^3 S_1^{[1]} + {}^3 S_1^{[1]}$	$R_1 = R_2 = -\frac{11}{6}$	${}^1 S_0^{[1]} + {}^1 S_0^{[1]}$	$R_1 = R_2 = -\frac{1}{2}$		

### VIII. ACKNOWLEDGEMENTS:

The authors would like to thank Dr. Guang-Yu Wang for providing the code of NLO radiative corrections for  $J/\psi$  pair production. This work was supported by the National Natural Science Foundation of China (No 11705078).

- 
- [1] G. T. Bodwin, E. Braaten, and G. P. Lepage, Rigorous qcd analysis of inclusive annihilation and production of heavy quarkonium, *Physical Review D* **51**, 1125 (1995).
  - [2] G. T. Bodwin, E. Braaten, T. C. Yuan, and G. P. Lepage, P-wave charmonium production in b-meson decays, *Physical Review D* **46**, R3703 (1992).
  - [3] F. Abe, H. Akimoto, A. Akopian, M. Albrow, S. Amendolia, D. Amidei, J. Antos, S. Aota, G. Apollinari, T. Asakawa, et al.,  $J/\psi$  and  $\psi(2s)$  production in  $p p^-$  collisions at  $\sqrt{s} = 1.8$  tev, *Physical review letters* **79**, 572 (1997).
  - [4] F. Abe, H. Akimoto, A. Akopian, M. Albrow, S. Amendolia, D. Amidei, J. Antos, S. Aota, G. Apollinari, T. Asakawa, et al., Production of  $j/\psi$  mesons from  $\chi c$  meson decays in  $p p^-$  collisions at  $\sqrt{s} = 1.8$  tev, *Physical review letters* **79**, 578 (1997).
  - [5] E. Braaten and S. Fleming, Color-octet fragmentation and the  $\psi'$  surplus at the fermilab tevatron, *Physical Review Letters* **74**, 3327 (1995).
  - [6] M. Butenschoen and B. A. Kniehl, World data of  $j/\psi$  production consolidate nonrelativistic qcd factorization? format?; at next-to-leading order, *Physical Review D* **84**, 051501 (2011).
  - [7] K.-T. Chao, Y.-Q. Ma, H.-S. Shao, K. Wang, and Y.-J. Zhang,  $J/\psi$  polarization at hadron colliders in nonrelativistic qcd, *Physical review letters* **108**, 242004 (2012).
  - [8] B. Gong, L.-P. Wan, J.-X. Wang, and H.-F. Zhang, Polarization for prompt  $j/\psi$  production at the tevatron and lhc, *Physical review letters* **110**, 042002 (2013).
  - [9] G. T. Bodwin, H. S. Chung, U.-R. Kim, and J. Lee, Fragmentation contributions to  $j/\psi$  production at the tevatron and the lhc, *Physical review letters* **113**, 022001 (2014).
  - [10] K. Abe, K. Abe, H. Aihara, Y. Asano, V. Aulchenko, T. Aushev, S. Bahinipati, A. Bakich, Y. Ban, I. Bedny, et al., Study of double charmonium production in  $e^+ e^-$  annihilation at  $s = 10.6$  g e v, *Physical Review D* **70**, 071102 (2004).
  - [11] B. Aubert, R. Barate, D. Boutigny, F. Couderc, Y. Karyotakis, J. Lees, V. Poireau, V. Tisserand, A. Zghiche, E. Grauges, et al., Measurement of double charmonium production in  $e^+ e^-$  annihilations at  $s = 10.6$  gev, *Physical Review D* **72**, 031101 (2005).
  - [12] K.-Y. Liu, Z.-G. He, and K.-T. Chao, Problems of double-charm production in  $e^+ e^-$  annihilation at  $s = 10.6$  gev, *Physics Letters B* **557**, 45 (2003).
  - [13] E. Braaten and J. Lee, Exclusive double-charmonium production from  $e^+ e^-$  annihilation into a virtual photon, *Physical Review D* **67**, 054007 (2003).
  - [14] K. Hagiwara, E. Kou, and C.-F. Qiao, Exclusive  $j/\psi$  productions at  $e^+ e^-$  colliders, *Physics Letters B* **570**, 39 (2003).
  - [15] Y.-J. Zhang, Y.-J. Gao, and K.-T. Chao, Next-to-leading-order qcd correction to  $e^+ e^- \rightarrow j/\psi + \eta c$  at  $s = 10.6$  gev, *Physical review letters* **96**, 092001 (2006).
  - [16] B. Gong and J.-X. Wang, Qcd corrections to  $j/\psi$  plus  $\eta c$  production in  $e^+ e^-$  annihilation at  $s = 10.6$  gev, *Physical Review D* **77**, 054028 (2008).
  - [17] Z.-G. He, Y. Fan, and K.-T. Chao, Relativistic corrections to  $j/\psi$  exclusive and inclusive double charm production at b

- factories, *Physical Review D* **75**, 074011 (2007).
- [18] Y. Jia, Color-singlet relativistic correction to inclusive  $j/\psi$  production associated with light hadrons at b factories, *Physical Review D* **82**, 034017 (2010).
- [19] Z.-G. He, Y. Fan, and K.-T. Chao, Relativistic correction to  $e^+e^- \rightarrow j/\psi + gg$  at b factories and constraint on color-octet matrix elements, *Physical Review D* **81**, 054036 (2010).
- [20] G. T. Bodwin, J. Lee, and C. Yu, Resummation of relativistic corrections to  $e^+e^- \rightarrow j/\psi + \eta_c$ , *Physical Review D* **77**, 094018 (2008).
- [21] H.-R. Dong, F. Feng, and Y. Jia,  $O(\alpha_s v^2)$  correction to  $e^+e^- \rightarrow J/\psi + \eta_c$  at B factories, *Phys. Rev. D* **85**, 114018 (2012), [arXiv:1204.4128 \[hep-ph\]](#).
- [22] X.-D. Huang, B. Gong, and J.-X. Wang, Next-to-next-to-leading-order QCD corrections to  $J/\psi$  plus  $\eta_c$  production at the B factories, *JHEP* **02**, 049, [arXiv:2212.03631 \[hep-ph\]](#).
- [23] N. Brambilla et al., Heavy Quarkonium: Progress, Puzzles, and Opportunities, *Eur. Phys. J. C* **71**, 1534 (2011), [arXiv:1010.5827 \[hep-ph\]](#).
- [24] A. Andronic et al., Heavy-flavour and quarkonium production in the LHC era: from proton–proton to heavy-ion collisions, *Eur. Phys. J. C* **76**, 107 (2016), [arXiv:1506.03981 \[nucl-ex\]](#).
- [25] H. S. Chung, Review of quarkonium production: status and prospects, *PoS Confinement2018*, 007 (2018), [arXiv:1811.12098 \[hep-ph\]](#).
- [26] A.-P. Chen, Y.-Q. Ma, and H. Zhang, A Short Theoretical Review of Charmonium Production, *Adv. High Energy Phys.* **2022**, 7475923 (2022), [arXiv:2109.04028 \[hep-ph\]](#).
- [27] E. Chapon et al., Prospects for quarkonium studies at the high-luminosity LHC, *Prog. Part. Nucl. Phys.* **122**, 103906 (2022), [arXiv:2012.14161 \[hep-ph\]](#).
- [28] M. Dong et al. (CEPC Study Group), CEPC Conceptual Design Report: Volume 2 - Physics & Detector, (2018), [arXiv:1811.10545 \[hep-ex\]](#).
- [29] I. Agapov et al., Future Circular Lepton Collider FCC-ee: Overview and Status, in *Snowmass 2021* (2022) [arXiv:2203.08310 \[physics.acc-ph\]](#).
- [30] M. Koratzinos (FCC-ee study), FCC-ee accelerator parameters, performance and limitations, *Nucl. Part. Phys. Proc.* **273-275**, 2326 (2016), [arXiv:1411.2819 \[physics.acc-ph\]](#).
- [31] G. Aarons et al. (ILC), International Linear Collider Reference Design Report Volume 2: Physics at the ILC, (2007), [arXiv:0709.1893 \[hep-ph\]](#).
- [32] J. Erler, S. Heinemeyer, W. Hollik, G. Weiglein, and P. M. Zerwas, Physics impact of GigaZ, *Phys. Lett. B* **486**, 125 (2000), [arXiv:hep-ph/0005024](#).
- [33] J. A. Aguilar-Saavedra et al. (ECFA/DESY LC Physics Working Group), TESLA: The Superconducting electron positron linear collider with an integrated x-ray laser laboratory. Technical design report. Part 3. Physics at an  $e^+e^-$  linear collider, (2001), [arXiv:hep-ph/0106315](#).
- [34] J. Erler, S. Heinemeyer, W. Hollik, G. Weiglein, and P. M. Zerwas, Physics impact of GigaZ, *Phys. Lett. B* **486**, 125 (2000), [arXiv:hep-ph/0005024](#).
- [35] J.-P. Ma and Z.-X. Zhang, Preface, *Sci. Chin. Phys. Mech. Astro.* **53**, 1947 (2010).
- [36] G. Chen, X.-G. Wu, Z. Sun, S.-Q. Wang, and J.-M. Shen, Exclusive charmonium production from  $e^+e^-$  annihilation round the  $Z^0$  peak, *Phys. Rev. D* **88**, 074021 (2013), [arXiv:1308.5375 \[hep-ph\]](#).
- [37] A. K. Likhoded and A. V. Luchinsky, Double Charmonia Production in Exclusive Z Boson Decays, *Mod. Phys. Lett. A* **33**, 1850078 (2018), [arXiv:1712.03108 \[hep-ph\]](#).
- [38] A. V. Berezhnoy, I. N. Belov, S. V. Poslavsky, and A. K. Likhoded, One-loop corrections to the processes  $e^+e^- \rightarrow \gamma$ ,  $Z \rightarrow J/\psi \eta_c$  and  $e^+e^- \rightarrow Z \rightarrow J/\psi J/\psi$ , *Phys. Rev. D* **104**, 034029 (2021), [arXiv:2101.01477 \[hep-ph\]](#).
- [39] X. Luo, H.-B. Fu, H.-J. Tian, and C. Li, Next-to-leading-order QCD correction to the exclusive double charmonium production via Z decays, (2022), [arXiv:2209.08802 \[hep-ph\]](#).
- [40] I. N. Belov, A. V. Berezhnoy, and E. A. Leshchenko, Associated Quarkonia Production in a Single Boson  $e^+e^-$  Annihilation, *Phys. Atom. Nucl.* **86**, 1474 (2023), [arXiv:2303.03362 \[hep-ph\]](#).
- [41] A. V. Berezhnoy, A. K. Likhoded, A. I. Onishchenko, and S. V. Poslavsky, Next-to-leading order QCD corrections to paired Bc production in  $e^+e^-$  annihilation, *Nucl. Phys. B* **915**, 224 (2017), [arXiv:1610.00354 \[hep-ph\]](#).
- [42] I. N. Belov, A. Berezhnoy, and E. Leshchenko, Associated Charmonium–Bottomonium Production in a Single Boson  $e^+e^-$  Annihilation, *Symmetry* **13**, 1262 (2021), [arXiv:2105.06174 \[hep-ph\]](#).
- [43] Q.-L. Liao, J. Jiang, and Y.-H. Zhao, Production of double heavy quarkonia at super z factory, *The European Physical Journal C* **83**, 10.1140/epjc/s10052-023-11174-x (2023).
- [44] Q.-L. Liao and J. Jiang, Production of higher excited quarkonium pair at the super Z factory, *Chin. Phys. C* **48**, 073102 (2024).
- [45] Q.-L. Liao, J. Jiang, and Y.-H. Zhao, Production of double P-wave heavy quarkonia at a super Z factory, *Eur. Phys. J. C* **83**, 22 (2023), [arXiv:2206.06123 \[hep-ph\]](#).
- [46] Z. Sun, X.-G. Wu, G. Chen, J. Jiang, and Z. Yang, Heavy quarkonium production through the semi-exclusive  $e^+e^-$  annihilation channels round the  $Z^0$  peak, *Phys. Rev. D* **87**, 114008 (2013), [arXiv:1302.4282 \[hep-ph\]](#).
- [47] T. Hahn, Generating Feynman diagrams and amplitudes with FeynArts 3, *Comput. Phys. Commun.* **140**, 418 (2001), [arXiv:hep-ph/0012260](#).
- [48] R. Mertig, M. Bohm, and A. Denner, FEYN CALC: Computer algebraic calculation of Feynman amplitudes, *Comput. Phys. Commun.* **64**, 345 (1991).
- [49] Y.-J. Li, G.-Z. Xu, K.-Y. Liu, and Y.-J. Zhang, Relativistic Correction to J/psi and Upsilon Pair Production, *JHEP* **07**, 051,

- arXiv:1303.1383 [hep-ph].
- [50] Y.-J. Li, G.-Z. Xu, K.-Y. Liu, and Y.-J. Zhang, Search for  $C = +$  charmonium and XYZ states in  $e^+e^- \rightarrow \gamma + H$  at BESIII, *JHEP* **01**, 022, arXiv:1310.0374 [hep-ph].
- [51] M. Tanabashi et al. (Particle Data Group), Review of Particle Physics, *Phys. Rev. D* **98**, 030001 (2018).
- [52] G.-M. Yu, Y.-B. Cai, Y.-D. Li, and J.-S. Wang, Heavy quarkonium photoproduction in ultrarelativistic heavy ion collisions, *Phys. Rev. C* **95**, 014905 (2017), [Addendum: *Phys.Rev.C* 95, 069901 (2017)], arXiv:1703.03194 [hep-ph].
- [53] G. T. Bodwin and J. Lee, Relativistic corrections to gluon fragmentation into spin triplet S wave quarkonium, *Phys. Rev. D* **69**, 054003 (2004), arXiv:hep-ph/0308016.
- [54] M. Gremm and A. Kapustin, Annihilation of S wave quarkonia and the measurement of  $\alpha_s$ , *Phys. Lett. B* **407**, 323 (1997), arXiv:hep-ph/9701353.
- [55] P. L. Cho and A. K. Leibovich, Color octet quarkonia production, *Phys. Rev. D* **53**, 150 (1996), arXiv:hep-ph/9505329.
- [56] P. L. Cho and A. K. Leibovich, Color octet quarkonia production. 2., *Phys. Rev. D* **53**, 6203 (1996), arXiv:hep-ph/9511315.
- [57] M. Butenschoen, Z.-G. He, and B. A. Kniehl,  $\eta_c$  production at the LHC challenges nonrelativistic-QCD factorization, *Phys. Rev. Lett.* **114**, 092004 (2015), arXiv:1411.5287 [hep-ph].
- [58] H. Han, Y.-Q. Ma, C. Meng, H.-S. Shao, and K.-T. Chao,  $\eta_c$  production at LHC and indications on the understanding of  $J/\psi$  production, *Phys. Rev. Lett.* **114**, 092005 (2015), arXiv:1411.7350 [hep-ph].
- [59] H.-F. Zhang, Z. Sun, W.-L. Sang, and R. Li, Impact of  $\eta_c$  hadroproduction data on charmonium production and polarization within NRQCD framework, *Phys. Rev. Lett.* **114**, 092006 (2015), arXiv:1412.0508 [hep-ph].
- [60] Z.-G. He and B. A. Kniehl, Complete Nonrelativistic-QCD Prediction for Prompt Double  $J/\psi$  Hadroproduction, *Phys. Rev. Lett.* **115**, 022002 (2015), arXiv:1609.02786 [hep-ph].
- [61] J.-X. Wang and H.-F. Zhang,  $h_c$  production at hadron colliders, *J. Phys. G* **42**, 025004 (2015), arXiv:1403.5944 [hep-ph].
- [62] E. Braaten, S. Fleming, and A. K. Leibovich, NRQCD analysis of bottomonium production at the Tevatron, *Phys. Rev. D* **63**, 094006 (2001), arXiv:hep-ph/0008091.
- [63] R. Sharma and I. Vitev, High transverse momentum quarkonium production and dissociation in heavy ion collisions, *Phys. Rev. C* **87**, 044905 (2013), arXiv:1203.0329 [hep-ph].
- [64] J. L. Domenech and M. A. Sanchis-Lozano, Bottomonium production at the Tevatron and the LHC, *Phys. Lett. B* **476**, 65 (2000), arXiv:hep-ph/9911332.
- [65] E. J. Eichten and C. Quigg, Quarkonium wave functions at the origin, *Phys. Rev. D* **52**, 1726 (1995), arXiv:hep-ph/9503356.
- [66] W. Buchmuller and S. H. H. Tye, Quarkonia and Quantum Chromodynamics, *Phys. Rev. D* **24**, 132 (1981).
- [67] K. Igi and S. Ono, Heavy Quarkonium Systems and the QCD Scale Parameter  $\Lambda$  Ms, *Phys. Rev. D* **33**, 3349 (1986).
- [68] Q.-L. Liao and G.-Y. Xie, Heavy quarkonium wave functions at the origin and excited heavy quarkonium production via top quark decays at the LHC, *Phys. Rev. D* **90**, 054007 (2014), arXiv:1408.5563 [hep-ph].
- [69] Y.-Q. Chen and Y.-P. Kuang, Improved QCD motivated heavy quark potentials with explicit  $\Lambda$ (ms) dependence, *Phys. Rev. D* **46**, 1165 (1992), [Erratum: *Phys.Rev.D* 47, 350 (1993)].
- [70] Y.-J. Zhang, B.-Q. Li, and K.-Y. Liu,  $J/\psi$  electromagnetic production associated with light hadrons at  $B$  factories, (2010), arXiv:1003.5566 [hep-ph].
- [71] A. Trunin, Resummation of relativistic corrections to heavy quarkonium  $+\gamma$  production at  $Z$  factory, (2024), arXiv:2406.05729 [hep-ph].
- [72] S. Bhatnagar and H. Negash, ( $J/\psi, J/\psi$ ), and ( $\eta_c, \eta_c$ ) production through two intermediate photons in electron-positron annihilation at B-factories, *Nucl. Phys. A* **1053**, 122969 (2025), arXiv:2406.07508 [hep-ph].
- [73] X.-C. Zheng, C.-H. Chang, X.-G. Wu, X.-D. Huang, and G.-Y. Wang, Inclusive production of heavy quarkonium  $\eta_Q$  via  $Z$  boson decays within the framework of nonrelativistic QCD, *Phys. Rev. D* **104**, 054044 (2021), arXiv:2104.03808 [hep-ph].
- [74] K.-Y. Liu, Z.-G. He, and K.-T. Chao, Search for excited charmonium states in  $e^+e^-$  annihilation at  $s^{**}(1/2) = 10.6\text{-GeV}$ , *Phys. Rev. D* **77**, 014002 (2008), arXiv:hep-ph/0408141.
- [75] M. Beneke and M. Krämer, Direct  $J/\psi$  and  $\psi'$  polarization and cross-sections at the Tevatron, *Phys. Rev. D* **55**, 5269 (1997), arXiv:hep-ph/9611218.
- [76] E. Braaten, B. A. Kniehl, and J. Lee, Polarization of prompt  $J/\psi$  at the Tevatron, *Phys. Rev. D* **62**, 094005 (2000), arXiv:hep-ph/9911436.
- [77] G. T. Bodwin, H. S. Chung, U.-R. Kim, and J. Lee, Fragmentation contributions to  $J/\psi$  production at the Tevatron and the LHC, *Phys. Rev. Lett.* **113**, 022001 (2014), arXiv:1403.3612 [hep-ph].
- [78] S. Fleming and T. Mehen, Photoproduction of  $h(c)$ , *Phys. Rev. D* **58**, 037503 (1998), arXiv:hep-ph/9801328.
- [79] E. Braaten, S. Fleming, and T. C. Yuan, Production of heavy quarkonium in high-energy colliders, *Ann. Rev. Nucl. Part. Sci.* **46**, 197 (1996), arXiv:hep-ph/9602374.
- [80] M. Beneke, F. Maltoni, and I. Z. Rothstein, QCD analysis of inclusive B decay into charmonium, *Phys. Rev. D* **59**, 054003 (1999), arXiv:hep-ph/9808360.
- [81] Y. Jia, W.-L. Sang, and J. Xu, Inclusive  $h_c$  Production at  $B$  Factories, *Phys. Rev. D* **86**, 074023 (2012), arXiv:1206.5785 [hep-ph].
- [82] M. Beneke and M. Krämer, Direct  $J/\psi$  and  $\psi'$  polarization and cross-sections at the Tevatron, *Phys. Rev. D* **55**, 5269 (1997), arXiv:hep-ph/9611218.
- [83] G. T. Bodwin, E. Braaten, T. C. Yuan, and G. P. Lepage, P wave charmonium production in B meson decays, *Phys. Rev. D* **46**, R3703 (1992), arXiv:hep-ph/9208254.
- [84] H.-S. Shao, Y.-Q. Ma, K. Wang, and K.-T. Chao, Polarizations of  $\chi_{c1}$  and  $\chi_{c2}$  in prompt production at the LHC, *Phys. Rev. Lett.* **112**, 182003 (2014), arXiv:1402.2913 [hep-ph].



- [85] Y.-J. Zhang, Y.-Q. Ma, K. Wang, and K.-T. Chao, QCD radiative correction to color-octet  $J/\psi$  inclusive production at B Factories, *Phys. Rev. D* **81**, 034015 (2010), [arXiv:0911.2166 \[hep-ph\]](#).
- [86] G.-Z. Xu, Y.-J. Li, K.-Y. Liu, and Y.-J. Zhang, Relativistic Correction to Color Octet  $J/\psi$  Production at Hadron Colliders, *Phys. Rev. D* **86**, 094017 (2012), [arXiv:1203.0207 \[hep-ph\]](#).
- [87] G.-Z. Xu, Y.-J. Li, K.-Y. Liu, and Y.-J. Zhang,  $\alpha_s v^2$  corrections to  $\eta_c$  and  $\chi_{cJ}$  production recoiled with a photon at  $e^+e^-$  colliders, *JHEP* **10**, 071, [arXiv:1407.3783 \[hep-ph\]](#).